Journal of Hydrology: Regional Studies 62 (2025) 103015

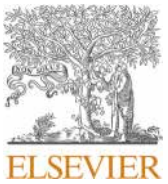

Contents lists available at ScienceDirect

Journal of Hydrology: Regional Studies

journal homepage: www.elsevier.com/locate/ejrh

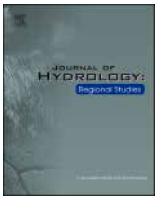

Investigating hydrological modeling uncertainties in the Mediterranean region by combining precipitation and soil moisture products

Vianney Sivelle [a,b,*], Christian Massari [a], Yves Tramblay [c], Paolo Filippucci [a], Hamouda Dakhlaoui [d,e], Pere Quintana-Seguí [f], Roger Clavera-Gispert [f], Hamouda Boutaghane [g], Tayeb Boulmaiz [h], Raphael Quast [i], Mariette Vreugdenhill [i]

[a] Research Institute for Geo-Hydrological Protection, National Research Council, Perugia, Italy
[b] HSM, Univ Montpellier, CNRS, IRD, Montpellier, France
[c] Espace-Dev, Univ. Montpellier, IRD, Montpellier, France
[d] LMHE, Ecole Nationale d'Ingénieurs de Tunis, Université Tunis El Manar, BP37, Tunis Le Belvedère 1002, Tunisia
[e] Ecole Nationale d'Architecture et d'Urbanisme, Université de Carthage, Sidi Bou Said, Tunisia
[f] Observatori de l'Ebre (OE), Ramon Llull University, CSIC, Roquetes 43520, Spain
[g] Laboratory of hydraulics and hydraulic constructions, Badji Mokhtar University, Algeria
[h] Materials, Energy Systems Technology and Environment Laboratory, Université de Ghardaia, Ghardaia, Algeria
[i] TU Wien, Department of Geodesy and Geoinformation, Vienna, Austria

ARTICLE INFO

Keywords:
Hydrological modeling
Precipitation
Soil moisture
Earth observation
Satellite precipitation Product

ABSTRACT

Study region: The study focus on five catchments in the Mediterranean Region distributed over Spain, France, Italy, Tunisia and Algeria.
Study focus: The study runs four lumped parameter hydrological models combining eight precipitation products and four soil moisture products. A Bayesian inference scheme is built to estimate posterior parameter distribution for any combination of hydrological model, precipitation and soil moisture. The simulated streamflows are evaluated using both Nash-Sutcliffe Efficiency criteria and multi-resolution analysis. The results from Bayesian inference combining streamflow and soil moisture is compared to the results when considering only streamflow as a benchmark.
New hydrological insights for the region: The results indicates that hydrological model performance through the Nash-Sutcliffe Efficiency criteria is more sensitive to the forcing precipitation product than the model structure. Also, forcing hydrological models with merged precipitation product brings better streamflow predictions than using satellite precipitation products. Regarding soil moisture accounting in hydrological modeling, the results show that including soil moisture in the parameter estimation can improve the predictive performance of hydrological models when the model is forced with satellite precipitation product. Also, soil moisture datasets derived from Sentinel-1 offer better consistency in hydrological modeling of river streamflow simulation.

* Corresponding author at: Research Institute for Geo-Hydrological Protection, National Research Council, Perugia, Italy.
E-mail address: vianney.sivelle@umontpellier.fr (V. Sivelle).

https://doi.org/10.1016/j.ejrh.2025.103015
Received 10 June 2025; Received in revised form 13 November 2025; Accepted 1 December 2025
Available online 3 December 2025

1. Introduction

Hydrological Models (HM) aim to establish streamflow predictions using meteorological forcing data (i.e., precipitation, temperature, potential evapotranspiration). The predictive performance of HMs relies on the model structure (Gupta and Govindaraju, 2019; Knoben et al., 2020; Refsgaard et al., 2006; Renard et al., 2010), the calibration procedure (Herrera et al., 2022; Siebert et al., 2010), the forcing data (Oudin et al., 2006) as well as the initial conditions (Mazzilli et al., 2012). HMs are generally designed based on a prior conceptualization of the flow behavior within the catchment of interest (McMillan et al., 2023) while the parameter estimation is performed with history matching based on field observations (Klemeš, 1986; Seibert, 2001). Model calibration aims at finding the model parameters values allowing them to better reproduce the field observations. In most hydrological studies, history matching is performed regarding streamflow times series alone. Various studies have shown an interest in considering complementary observations for history matching such as piezometric head (Cousquer and Jourde, 2022; Flinck et al., 2021; Lamb et al., 1998; Seibert, 2000), soil moisture (Eini et al., 2023; Shahrban et al., 2018; Tong et al., 2022), physicochemical parameters (Schilling et al., 2019) or actual evapotranspiration (Bargaoui et al., 2008). Complementary observations allow investigating both explanatory and predictive dimensions (Andréassian, 2023; Beven, 2001) of HMs thus allowing to investigate if model predictions can be considered satisfactory for suitable reasons. While the main goal of HMs consists of providing streamflow predictions, the consistency of HMs can be evaluated regarding various components of the water stocks and fluxes such as (i) the hydrodynamics within the unsaturated zone through the soil moisture dynamics, and (ii) the interaction within the soil-vegetation-atmosphere continuum through the actual evapotranspiration. Then, the water balance within the various compartments of HMs allows to better assess the contribution of the catchment of interest within the terrestrial water cycle. Also, the development of new Earth Observation (EO) data such as those from the Sentinel-1 mission offers new constraints for HMs (Bechtold et al., 2023; Cenci et al., 2017) leading to better consistency in hydrological modeling but also bring additional potential uncertainty in the hydrological modeling chain (Maggioni and Massari, 2018).

While precipitation data is essential for HMs, the high variability in time and space makes it difficult to get suitable precipitation time series for catchment scale hydrological modeling, particularly in data-scarce regions. Among the various types of HMs, lumped parameter HMs consist of a functional approach that analyzes a hydro(geo)logical system at the catchment scale and describes the transformation from precipitation into streamflow using empirical or conceptual relationships. The forcing dataset consists of precipitated water that can be estimated based on either a meteorological ground station (assuming the station to be representative of the catchment) or a distributed precipitation dataset (e.g., interpolated ground station data or radar-derived precipitation). Ground-station measurements are the most reliable source of precipitation (direct measurement over data-dense regions) although some modeling exercises have shown that using integrated precipitation products can outperform the use of ground-station data (Camici et al., 2018). Recent studies have investigated the use of either reanalysis products or satellite precipitation products (SPP) in place of classical gauge measurement for hydrological modeling (Maggioni and Massari, 2018). Tramblay et al. (2023b) showed that using SM2RAIN precipitation products can reach satisfactory results for daily hydrological modeling in Morocco. Cantoni et al. (2022) used ERA5 for flood modeling in Tunisia. The authors showed that it can be a valuable alternative to observed precipitation as long as parameter estimation for HM can be performed with streamflow observations. Ciabatta et al. (2016) forced the MISDc model (Brocca et al., 2011; Massari et al., 2018) with both ground observed precipitation and SPP. The results showed that the use of SPP for daily discharge simulation requires a parameter estimation procedure to obtain consistent hydrological predictions over four catchments in Italy. While SPPs suffer from biases, they can still well capture the temporal variability of precipitation at the catchment scale (Nikolopoulos et al., 2013; Stampoulis et al., 2013). Then, SPP-forced HMs require a parameter estimation procedure to substantially improve the model performance in hydrological modeling. Nonetheless, such an approach may introduce parametric uncertainty where HMs can compensate for SPP bias. Therefore, using a multi-HMs ensemble to evaluate SPP appears suitable for avoiding (or limiting) such SPP-HM compensation and should bring robustness to SPP evaluation.

Up to date, small and mesoscale applications in hydrological modeling get limited access to suitable satellite derived estimation of continental water cycle components, in particular precipitation and soil moisture. Indeed, most of the products offer coarse resolution that appears unsuitable for hydrological modeling over mesoscale catchments. The recent development in EO brings new estimation of continental water cycle component at 1 km of spatial resolution for precipitation (Filippucci et al., 2025, 2022) and soil moisture (Alfieri et al., 2022; Madelon et al., 2023; Quast et al., 2023). Only few studies investigate the potential added value of such high-resolution products in hydrological modeling of small to mesoscale. Al-Khoury et al. (2024) assessed downscaled precipitation products (1 km spatial resolution) for hydrological modeling of a karst catchment in mountainous regions, characterized with a recharge area of 13.2 km^2. The results showed that the precipitation downscaling do not significantly affect the spring discharge simulation compared with the original precipitation products.

In this study, high-resolution precipitation products are compared with widely used precipitation products (derived from either observations, reanalysis or satellite) and combined with soil-moisture accounting within lumped parameter hydrological modeling. This study aims to investigates how considering various precipitation and soil moisture products affect streamflow simulation. This study focuses on mesoscale catchments in the Mediterranean Region (MR) where the typical catchment size is estimated around 10^2–10^3 km^2 (Merheb et al., 2016; Tramblay et al., 2023a). Then, five catchments are considered for hydrological modeling using four lumped parameter HMs. Every single HM is calibrated in a Bayesian framework, considering any combination among thirteen precipitation products (forcing data) and four soil moisture products (observation data). The HMs calibration is performed considering (i) streamflow only and (ii) joint streamflow and soil moisture. The analysis of the model performance across the various combinations of HMs, precipitations datasets and soil moisture datasets allows investigating (i) the interaction between the selection of both HM and forcing precipitation dataset and its impact on the overall predictive uncertainties, (ii) the potential added value of considering soil moisture in HM calibration for both explanatory and predictive dimensions of HMs and (iii) a potential added value of considering a

merged precipitation product to compensate for lack of ground data and sub-optimality of classical state-of-the-art SPPs for streamflow simulation over mesoscale catchments in the MR. This analysis is crucial in regions where conventional meteorological ground stations are sparse (e.g., in developing countries, and remote locations).

2. Study areas and datasets

Five catchments are selected around the MR (Fig. 1) based on their catchment size, the data availability as well as the length of the record and the data quality. The selected catchments are considered mesoscale, with an order of magnitude of the catchment size around 10^2–10^3 km^2. This catchment sample is used to investigate the potential added values of high-resolution (1 km, 1 day) precipitation and soil moisture datasets for hydrological modeling via a lumped parameters approach. The five catchments are Arga river at Funes station (Spain), Herault river at Laroque station (France), Tiber River at Santa Lucia station (Italy), Medjerda river at Jendouba station (Tunisia) and Tafna river at Ben Behdel station (Algeria). In the following the various catchments will be referred to based on the river names. Table 1 summarizes the main characteristics of the five catchments.

The required dataset counts both forcing data (i.e., precipitation P and potential evapotranspiration PET) as well as observation data for history matching (i.e., streamflow Q and soil moisture SM). P is considered forcing data while SM is considered for history matching. The PET time series are computed with the Hargreaves-Samani methods (Hargreaves and Samani, 1982) using the daily minimum and maximum temperature from ERA5-Land.

2.1. Precipitation

The complete dataset counts height sources of daily precipitation datasets (Table 2), either based on ground-station measurement or remote sensed: (i) The Global Daily Unified Gauge-Based Analysis of Precipitation (Chen et al., 2008) with a spatial resolution of 0.5°, referred to as CPC. (ii) A land-only gridded daily observational dataset for precipitation based on observations from meteorological stations over Europe provided by the National Meteorological and Hydrological Services (NMHSs) and other data holding institutes (Cornes et al., 2018), referred to as E-OBS. (iii) The Global Precipitation Measurement (GPM) consists of a satellite mission in which data are unified based on the Integrated Multi-satellitE Retrievals (IMERG) (Huffman et al., 2019), referred to as IMERG-LR GPM. The spatial resolution is 0.1° and the temporal resolution is 30 min. Here, the late-run version of the dataset is adopted, characterized by 12–18 h latency. In this study, the precipitation data were accumulated to obtain daily precipitation measurements. (iv) The Climate Hazards Group InfraRed Precipitation with Station data, referred to as CHIRPS (Funk et al., 2015) incorporates 0.05° resolution satellite imagery with ground station data. (v) The Precipitation Estimation from Remotely Sensed Information Using Artificial Neural Networks-Climate Data Record, referred to as PERSIANN-CDR (Ashouri et al., 2015), incorporates Gridded Satellite (GridSat-B1) Infra-Red (IR) derived from merging International Satellite Cloud Climatology Project (ISCCP) B1 IR with Global Precipitation Climatology Project (GPCP) Monthly Analysis Product. The PERSIANN-CDR spatial resolution in 0.25°. (vi) rainfall product

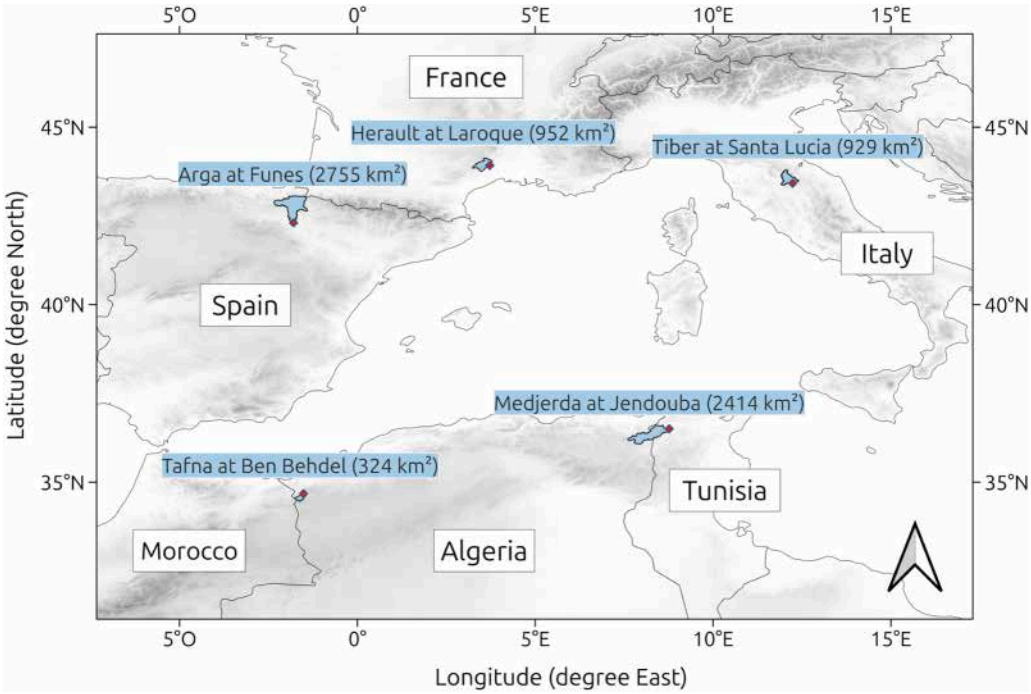

Fig. 1. Study sites located around the western part of the Mediterranean region. The red squares give the location of the gauging station.

Table 1
Information about the five catchments. The mean annual precipitation is estimated with CPC, ERA5-Land, IMERG-LR GPM and CPC-GPM-ASCAT time series. The mean annual potential evapotranspiration is estimated with Hargreaves-Samani (H-S) methods applied on ERA5-Land temperature. The land cover shown is the MCD12Q1.061 MODIS Land Cover Type 1 Yearly Global 500 m.

Name	Catchment area (km^2)	Mean annual precipitation (mm/year)	Mean annual potential evapotranspiration (mm/year)	Main land cover type
Arga Funes (Spain)	2755	862 (CPC) 934 (ERA5-Land) 1864 (IMERG-LR GPM) 838 (CPC-GPM-ASCAT)	918 (H-S)	Croplands (41 %) Deciduous broadleaf forest (17 %) Woody savannas (16 %)
Herault Laroque (France)	952	786 (CPC) 1168 (ERA5-Land) 1815 (IMERG-LR GPM) 911 (CPC-GPM-ASCAT)	957 (H-S)	Woody savannas (48 %) Savannas (19 %) Mixed forest (17 %)
Tiber Santa-Lucia (Italy)	929	793 (CPC) 1020 (ERA5-Land) 1795 (IMERG-LR GPM) 962 (CPC-GPM-ASCAT)	915 (H-S)	Woody savannas (37 %) Deciduous broadleaf forest (20 %)
Medjerda Jendouba (Tunisia)	2414	637 (CPC) 548 (ERA5-Land) 595 (CPC-GPM-ASCAT)	1284 (H-S)	Croplands (78 %) Grasslands (10 %)
Tafna Ben Behdel (Algeria)	324	254 (CPC) 404 (ERA5-Land) 675 (IMERG-LR GPM) 328 (CPC-GPM-ASCAT)	1294 (H-S)	Open shrublands (85 %) Grasslands (15 %)

Table 2
Precipitation products used as forcing data for the lumped parameter hydrological modeling exercise.

Notation	Spatial resolution	Original	Downscaled (1 km)
CPC	0.5 °	×	×
E-OBS	0.1 °	×	×
IMERG-LR GPM	0.1 °	×	×
CHIRPS	0.05 °	×	
PERSIANN-CDR	0.25 °	×	
SM2RAIN-ASCAT	0.1 °	×	×
ERA5-Land	0.1 °	×	×
CPC-GPM-ASCAT	1 km	×	

obtained from ASCAT soil moisture (Wagner et al., 2013) through the SM2RAIN algorithm (Brocca et al., 2019, 2014), referred to as SM2RAIN-ASCAT. The spatial resolution is 0.1°. (vii) The ERA5-Land reanalysis obtained by replaying the land component of the ECMWF ERA5 climate reanalysis at a 0.1° spatial resolution. (viii) 1km-scale precipitation that integrates CPC, IMERG-LR GPM and SM2RAIN-ASCAT precipitation datasets (Filippucci et al., 2024). The downscaling procedure is carried out by exploiting data from CHELSA climatology (Karger et al., 2021) that is used to distribute precipitation at the subpixel scale thus considering orographic enhancement (Filippucci et al., 2022). The corresponding dataset is referred to as CPC-GPM-ASCAT. In the present study, the various precipitation products are used either in their native spatial resolution or downscaled at 1 km resolution (Filippucci et al., 2023) so the overall precipitation datasets counts 13 precipitation datasets accounting for 8 precipitation datasets in their native resolution and 5 downscaled precipitation datasets (Table 2). In the following, the precipitation products are referred to with the given names, while the downscaled precipitation are referred to by the given name followed by the notation ‘ds’.

2.2. Soil moisture

The complete dataset counts four sources of soil moisture time series (Table 3): (i) The NASA-USDA Enhanced SMAP Global soil moisture data (Bolten et al., 2010; Entekhabi et al., 2010; Mladenova et al., 2017; Sazib et al., 2018), referred to as SMAP-SMP,

Table 3
Soil moisture products used as calibration data for lumped parameter hydrological modeling.

Notation	Spatial resolution	Temporal resolution
SMAP-SMP	10 km	1 day
TUWIEN-RT1	1 km	1–3 days
SMAP-Sentinel	3 km	1–3 days
GLEAM-SMroot	0.25 °	1 day

providing soil moisture profile at 10-km spatial sampling with a daily temporal resolution. The dataset is generated by integrating satellite-derived Soil Moisture Active Passive (SMAP) Level 2 soil moisture observations into the modified two-layer Palmer model using a 1-D Ensemble Kalman Filter data assimilation approach. (ii) The soil moisture data from Sentinel-1 C-band Synthetic Aperture Radar backscatter measurements using a radiative transfer modeling framework (Quast et al., 2023, 2019) referred to as TUWIEN-RT1. The spatial sampling is 500 m, and the temporal resolution is 1–3 days. (iii) The SMAP/Sentinel-1 L2 Radiometer/Radar 30 s Scene 3 km EASE-Grid Soil Moisture (Das et al., 2019), referred to as SMAP-Sentinel that provides estimates of land surface conditions retrieved by both the Soil Moisture Active Passive (SMAP) and Sentinel-1A and −1B radar. The spatial sampling is 3 km, and the temporal resolution is 1–3 days. (iv) The simulated root-zone soil moisture derived from the robust evapotranspiration scheme included in the Global Land Evaporation Amsterdam Model (GLEAM v3) (Miralles et al., 2011), referred to as GLEAM-SMroot. The latter have shown to be well correlated with runoff coefficient in Europe (Massari et al., 2023) and may support hydrological modeling. In this study, the soil moisture product are derived from stellite measurement, which nominally represent the moisture content within the top few centimeter of the soil layer (approximately 0–5 cm). However, the actual sensing depth can vary depending on soil texture, vegetation cover, and surface wetness conditions, and is often deeper under wet conditions (Feldman et al., 2023). In this study, rather than applying additional filtering or depth-scaling to the satellite soil moisture time series (e.g., Massari et al., 2015), the original observation are considered to preserve the temporal dynamics and to avoid the influence of inherent error of the observation into depth scaling parameters.

Soil moisture time series are built by averaging over the catchment of interest within each available time steps (Fig. 2). In order to avoid effect of bias in hydrological modeling, the soil moisture time series are normalized for 0–1, assuming that the catchment will face both dry and wet conditions over the period of interest. The missing time steps are not considered for hydrological modeling to avoid introducing falsification using interpolation for building continuous daily time series. Then, only available time steps are considered assuming the overall time series bring sufficient informative content for hydrological model calibration. The four soil moisture products show pretty close temporal dynamics alternating wet and dry periods, during extended winter and summer,

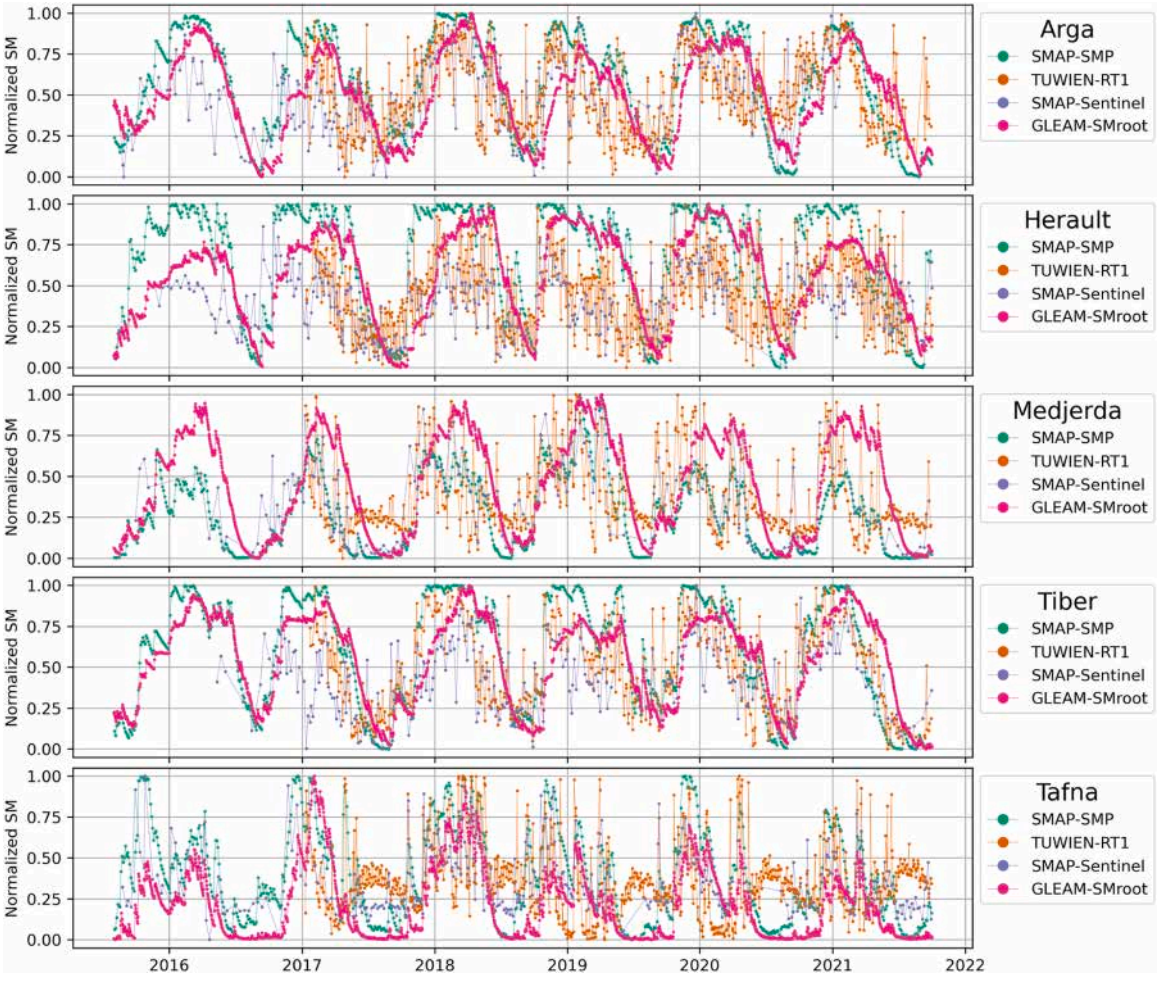

Fig. 2. Normalized soil moisture time series over tests sites considering four soil moisture products: SMAP-SMP, TUWIEN-RT1, SMAP-Sentinel and GLEAM-SMroot.

respectively. The SMAP-SMP reach the saturation every year for the catchment in northern MR (Arga, Herault and Tiber) showing long periods of saturation lasting up to months. Both SMAP-SMP and GLEAM-SMRoot show a low variability over short term scales while Sentinel-1 derived soil moisture (SMAP-Sentinel and TUWIEN-RT1) show significant variability. TUWIEN-RT1 seems to overestimate soil moisture during summer within both Medjerda and Tafna compared with the other soil moisture products. The overestimation of soil moisture in semi-arid regions is a well-known issue with soil moisture retrievals from radar data, as described by Wagner et al. (2024), (2022) for soil moisture retrievals from the Metop Advanced SCATterometers (ASCAT). The study found that sub-surface scattering when the soil is dry leads to an increase in backscatter, which subsequently leads to high soil moisture in the retrieval algorithm. It is likely that a similar sub-surface mechanism occurs in the Medjerda and Tafna catchments. As shown in Wagner et al. (2024) the probability of subsurface scattering is slightly higher in the region of the Tafna and Medjerda catchments. This is observed in the time series of TUWIEN-RT1 soil moisture, where in the Tafna catchment shows a distinct increase in soil moisture during the dry summer period, whereas in the Medjerda catchment this is less pronounced.

3. Methodology

3.1. Hydrological models (HMs)

Fig. 3 shows the model structure for each of the four hydrological models (HMs) used in this study: (i) GR4J (Perrin et al., 2003), (ii) HBV (Bergström, 1992), (iii) HYMOD (Boyle et al., 2003; Moore, 1985) and (iv) MILc (Massari et al., 2018). These HMs have been widely used in hydrology and show pretty parsimonious patterns with a reasonable number of parameters (between 4 and 9 parameters). HMs are considered in a lumped approach, assuming a catchment scale water balance between P, ET, and flow routine within the model structure. Each model accounts for a soil moisture store, allowing the transformation of the meteorological forcing (i.e., P and PET) into net precipitation that infiltrates. HMs allow us to estimate the actual evapotranspiration (AET) based on the water balance computed at each time step. Table 4 summarizes the HMs model parameter as well as the range of the parameter space to

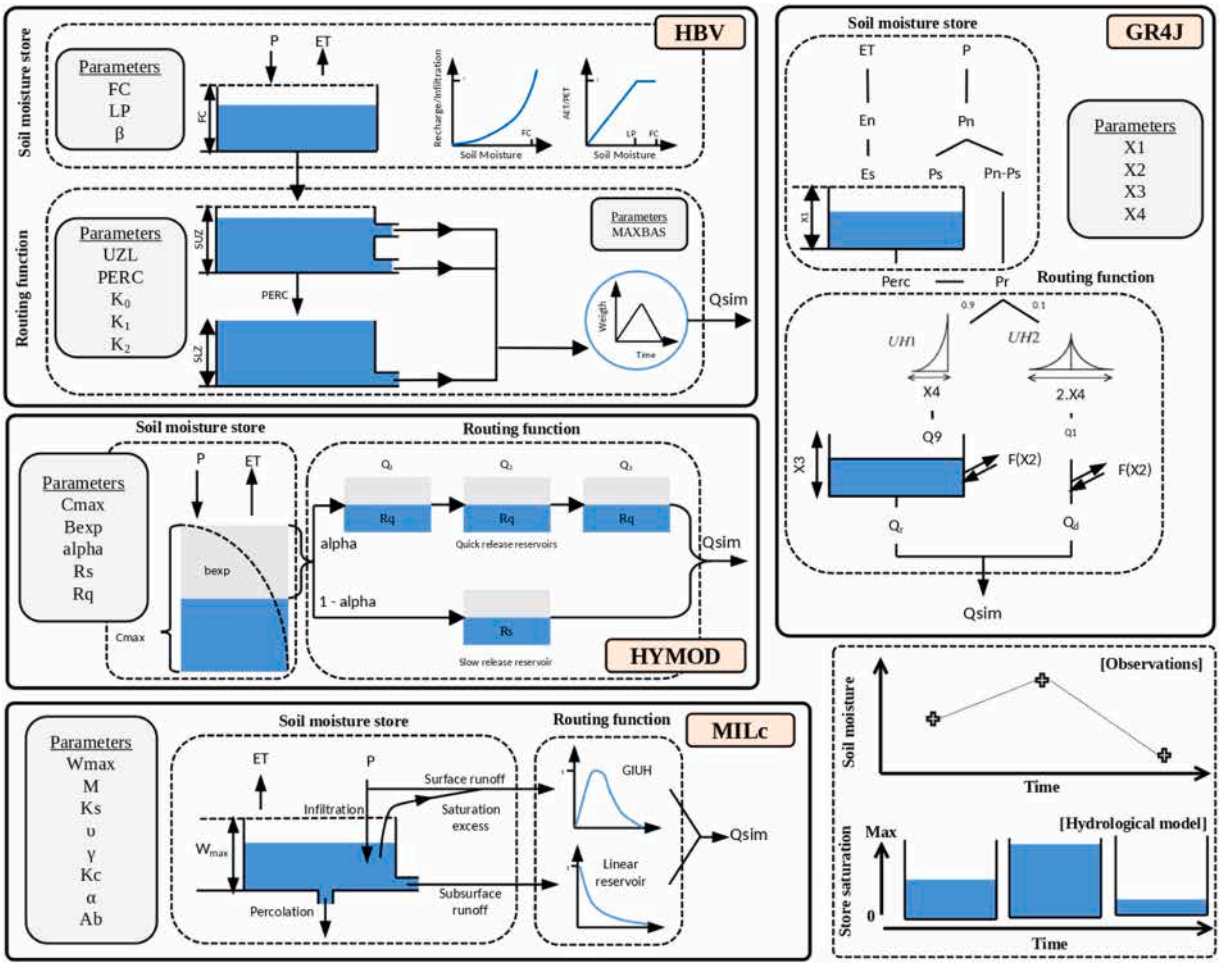

Fig. 3. Lumped parameter hydrological models: GR4J, HBV, HYMOD and MILc.

Table 4
Model parameters for hydrological models GR4J, HBV, HYMOD and MILc. Units are given for application of hydrological modeling on a daily temporal resolution.

Model	Parameter	Lower bound	Upper bound	Unit	Description
GR4J	X1	100	1200	mm	maximum capacity of the production store
	X2	-5	3	mm	groundwater exchange coefficient
	X3	20	300	mm	one day ahead maximum capacity of the routing store
	X4	1.1	2.9	day	time base of unit hydrograph UH1
HBV	BETA	1	6	mm	exponential parameter in soil routine
	LP	0.3	1	-	evapotranspiration limit
	FC	50	2000	mm	field capacity
	PERC	0	6	mm/day	maximum flux from Upper to Lower Zone
	K0	0.05	0.99	mm/day	near-surface flow coefficient
	K1	0.01	0.8	mm/day	upper Zone outflow coefficient
	K2	0.001	0.15	mm/day	lower Zone outflow coefficient
	UZL	0	100	mm	near-surface flow threshold
	MAXBAS	1	3	day	flow routing coefficient
HYMOD	Cmax	0	1000	mm	maximum storage capacity
	bexp	0	2	-	degree of spatial variability of the soil moisture capacity
	alpha	0.2	0.99	-	factor distributing the flow between slow and quick release reservoirs
	Rs	0.15	1.2	day	residence time of the slow-release reservoir
	Rq	0.01	0.15	day	residence time of the quick release reservoirs
MILc	W_p	0	1	-	initial conditions, fraction of W_{max}
	W*max*	50	1000	mm	field capacity
	m	2	10	-	exponent of drainage
	Ks	0.1	100	mm/day	coefficient for infiltration and drainage
	ν	0	2	-	fraction of drainage versus interflow
	γ	0.5	3.5	-	coefficient lag-time relationship
	Kc	0.4	2	-	parameter of potential evapotranspiration
	α	1	15	-	runoff exponent
	Ab	0.5	5	-	coefficient for Nash instantaneous Unit Hydrograph

investigate for the parameter estimation. These parameter ranges are given as prior for HM calibration regarding any combination of catchment, precipitation, and soil moisture datasets. Such a procedure allows the avoidance of bias related to the modeler's prior knowledge as well as limiting impacts of epistemic errors while investigating physical constraints on parameter range. The suggested parameter range is derived from literature (Table 4).

The GR4J model (Perrin et al., 2003) is a daily lumped parameter model with four parameters and consists of a production store and a routing store. The time lag between precipitation and streamflow is governed by two unit-hydrographs. The four model parameters are the maximum capacity of the production store (X1), a groundwater exchange coefficient (X2), the maximum capacity of the routing store (X3), and the time base of the unit hydrograph (X4). The precipitation P and potential evaporation PE are subtracted after interception to estimate the net rainfall P_n and the net evapotranspiration E_n.

The HBV model (Bergström, 1992) is originally a semi-distributed hydrological model, implemented here as a lumped parameter model, considering an unsaturated zone, an upper compartment and a lower compartment. The snow module is not considered since the study focuses only on precipitation-driven catchments. Therefore, the lumped HBV model used in this study counts nine parameters: the exponential parameter in soil routine (β), the evapotranspiration limit (LP), the field capacity (FC), the maximum flux from Upper to lower zone (PERC), the near-surface flow coefficient (k0), the upper Zone outflow coefficient (K1), the lower Zone outflow coefficient (K2), the near-surface flow threshold (UZL) and the flow routing coefficient (MAXBAS).

The HYMOD model (Quan et al., 2015) is a daily lumped parameter model based on the theory of runoff yield under excess infiltration. The HYMOD model counts five parameters: the maximum storage capacity (Cmax), the degree of spatial variability of the soil moisture capacity (Bexp), the factor distributing the flow between slow and quick release reservoirs (α), the residence time of the slow-release reservoir (Rs) and the residence time of the quick release reservoirs (Rq).

The MISDc model (Brocca et al., 2011; Massari et al., 2018) is originally a semi-distributed hydrological model, implemented here as a lumped parameter model, denoted MILc. The latter counts nine parameters: field capacity (W_{max}), initial conditions, as a fraction of W_{max} (W_p), the exponent of drainage (m), the coefficient of infiltration and drainage (Ks), the fraction of drainage versus interflow (ν), the coefficient lag-time relationship (γ), the parameter of potential evapotranspiration (Kc), the runoff exponent (α) and the Nash Instantaneous Unit Hydrograph (Ab).

3.2. Considering soil moisture in hydrological models

Soil moisture has been identified as a relevant proxy for hydrological behavior at the catchment scale, especially for runoff coefficient (Camici et al., 2022; Massari et al., 2023) as well as a precursor for flood events (Manoj J et al., 2023). Therefore, accounting for soil moisture in hydrological modeling has shown a significant added value for hydrological model performance and consistency (Alfieri et al., 2022; Koren et al., 2008; Shahrban et al., 2018; Wooldridge et al., 2003). As suggested by Shahrban et al. (2018), the simulated soil wetness SW_{sim} (%) is estimated for each time step *t* from the conceptual soil water store of HMs using:

$$SW_{\mathrm{sim,\,t}} = \frac{SM_{\mathrm{sim,\,t}}}{S_{\max}} \times 100 \tag{1}$$

where $SM_{sim,t}$ is the simulated soil moisture (mm) at time step t and S_{max} is the soil water storage (mm) in the HM. Therefore, S_{max} can be related to X1 in the GR4J model, FC in the HBV model, Cmax in the HYMOD model and W_{max} in the MILc model. Then, the simulated soil wetness can be compared to the various normalized soil moisture datasets (SMAP-SMP, TUWIEN-RT1, SMAP-Sentinel and GLEAM-SMroot, Fig. 2). The four HMs used in this study are based on a conceptual approach so the soil moisture helps constraining the temporal dynamic of the soil moisture store saturation but cannot be considered in terms of water volume. Nonetheless, temporal variability of soil moisture (and soil wetness in HMs) is hypothesized to be informative enough in order to support HMs calibration and counterbalance potential effect of errors in the precipitation time series. To evaluate this hypothesis, HMs are calibrated for any combination of precipitation and soil-moisture datasets.

3.3. Hydrological models calibration strategy

Bayesian inversion aims to approximate a *posterior* probability distribution on the parameter space and incorporates the noise in the measured discharge data as uncertainty in the estimated parameter distribution. The starting point in Bayesian inversion is a *prior* probability distribution that serves as a first guess on the distribution of the model parameters without considering any observations. This choice is often driven by intuition or expert knowledge. Here the *prior* is assumed as a uniform distribution bounded by a parameter space derived from the literature (Table 4). Observed and simulated system variable vectors are defined respectively by:

$$D = \{D_1, D_2, \ldots, D_n, \ldots, D_N\} \tag{2}$$

$$D^* = \{D_1^*, D_2^*, \ldots, D_n^*, \ldots, D_N^*\} \tag{3}$$

The likelihood function of model parameter ensemble P given the observations is represented by $L(P|D)$ which is defined by a normal likelihood function calculated for each simulator based on the agreement between the observed D and simulated system variable D*, here it is either streamflow or soil moisture time series or both, with a given precision τ:

$$L(P|D,\tau) = \sqrt{\frac{\tau}{2\pi}} \exp\left\{\frac{-\tau}{2}(D - D^*)^2\right\} \tag{4}$$

The error residuals are assumed normally distributed (mean=0 and standard deviation=5 % of the mean of the simulated time series). The system variable to be predicted is defined by Δ and with a distribution given by:

$$p(\Delta|D) = \sum_{j=1}^{J} p(\Delta \vee D) \tag{5}$$

In the case of parameter estimation, Δ is an element of observation vector D.

In this study, we use the a *Metropolis-Hastings algorithm* (Hastings, 1970) as an implementation of the *Marcov Chain Monte Carlo* (MCMC) sampling algorithm with the python package *pyMC* (Salvatier et al., 2016). The simulated time series used for the analysis consists of the meaning of an ensemble of 1000 simulated time series retrieved from the sampling of the *posterior* parameters' distributions. Then, the simulated time series considers an ensemble of model parameters. This avoids misinterpretation due to local optima and suggests better robustness of the HMs model performance. The methodology is applied for any combination of HM and precipitation dataset considering (i) only streamflow time series as observations and (ii) both streamflow and soil moisture time series as observations.

Due to data availability as well as for the sake of suitable model performance comparison using the various precipitation and soil moisture datasets, the calibration period is set from 01/08/2015–31/12/2021 (6 years and 5 months). This allows us to capture the variability within several hydrological years. All the variables of interest are available for the calibration periods except the soil moisture TUWIEN-RT1 starting from 2017. In this study we are not interested in the predictive capability of the different model, forcing and parameter configurations but on the impact of their uncertainty on the streamflow. Therefore, we have focused only on a calibration period (Arsenault et al., 2018). To understand the predictive performance of the different configurations data acquisition over a longer period will be necessary to perform classical split sample test (Klemeš, 1986).

3.4. Model performance evaluation

The metrics used for hydrological model calibration and evaluation are mainly based on the comparison between observed and simulated time series (Bennett et al., 2013; Ferreira et al., 2020; Hauduc et al., 2015; Jackson et al., 2019). To assess different aspects of the model performance, it is recommended to adopt a multi-objective model evaluation with a combination of different performance criteria (Huo and Liu, 2020; Monteil et al., 2020) since none of the existing metrics can reflect the overall rating behavior of humans (Gauch et al., 2022). Therefore, additional evaluation procedures may help to better capture how the model errors are structured in space (Thébault et al., 2023) and time (Molero et al., 2018). Here, the spatial patterns of model errors are not considered since the lumped parameters approach is considered for hydrological modeling. Among other performance criteria, the bounded version of the widely used Nash Sutcliff Efficiency (Mathevet et al., 2006; Nash and Sutcliffe, 1970) is used:

$$NSE = 1\frac{\sum (x_{\text{sim}} - x_{obs})^2}{\sum (x_{\text{obs}} - x_{obs})^2} \tag{6}$$

$$NSE_{c2m} = \frac{NSE}{2 - NSE} \tag{7}$$

Where x_{sim} and x_{obs} are respectively the simulated and the observed times series. The NSE compares the model performance of the model with the performance of a naïve predictor, which is the mean of the observed time series. The NSE_c2m offers the same benchmark, allowing us to discriminate if model performance is better than the naïve predictor when NSE_c2m > 0. Also, one should note that the suggested transformation leads to an NSE_c2m less optimistic for the positive values (Mathevet et al., 2006) but also reduce the data spreading with the negative NSE values. Using the NSE_c2m allows a more significant analysis on large number of model evaluations.

To investigate how the model errors are structured in time, the wavelet multiresolution analysis (MRA) is applied to project the streamflow time series on an orthogonal basis of wavelet and scale functions (Labat et al., 2000; Mallat, 1989). The basis is generated from a filter band following a dyadic scale, from 2 days (high frequency) up to 32 days (low frequency). The projection allows building for each temporal scale of the dyadic scale the component of the signal that explains the variability at this scale. The decomposition is orthogonal and therefore the sum of all components (details and residue) gives back the initial signal. Sivelle et al. (2022) applied MRA on both observed and simulated spring discharge time series of three karst catchments. By computing error metrics for each temporal scale, the author investigate how the structure of the model errors can be affected by the various modeling hypothesis. Here, the same procedure is performed to investigate how accounting for the various precipitation and soil moisture datasets affects the model errors across the various temporal scales. In the present study, the Pearson's correlation (Freedman et al., 2007) is considered to evaluate the simulated streamflow time series across the various temporal scales.

4. Results

4.1. Preliminary streamflow analysis

The five catchments share some relevant characteristics in terms of hydrological behavior (Fig. 4). First, the seasonality of the streamflow shows a characteristic "Mediterranean" pattern with a dry period during June-September and a wet season during the extended winter. The streamflow is not affected by snow melting at the end of the winter period. Also, the auto-correlation function ACF (Box et al., 2008) computed on the daily streamflow time series testify of quite low inertia of the hydro-system with a complete loss of the auto-correlation after around two months, showing that no long-term groundwater contribution can affect the river streamflow. Based on the cross-correlation function (CCF) analysis, the response time of each catchment has been estimated at around 1–2 days allowing a relevant time-space dimension to evaluate various precipitation datasets for lumped parameter hydrological modeling on a daily temporal resolution.

4.2. Precipitation evaluation

Fig. 5 shows the monthly cumulative precipitation and the cumulative probability distribution of the daily precipitation rate above the 95th percentile computed with the various precipitation datasets. IMERG-LR GPM overestimates the daily precipitation above the 95th percentile while the IMERG-LR GPM ds shows better agreement with observation (either CPC or E-OBS) for Herault and Tafna, or with CHIRPS for Arga and Medjerda. Both native and downscaled IMERG-LR GPM overestimates precipitation above the 95th

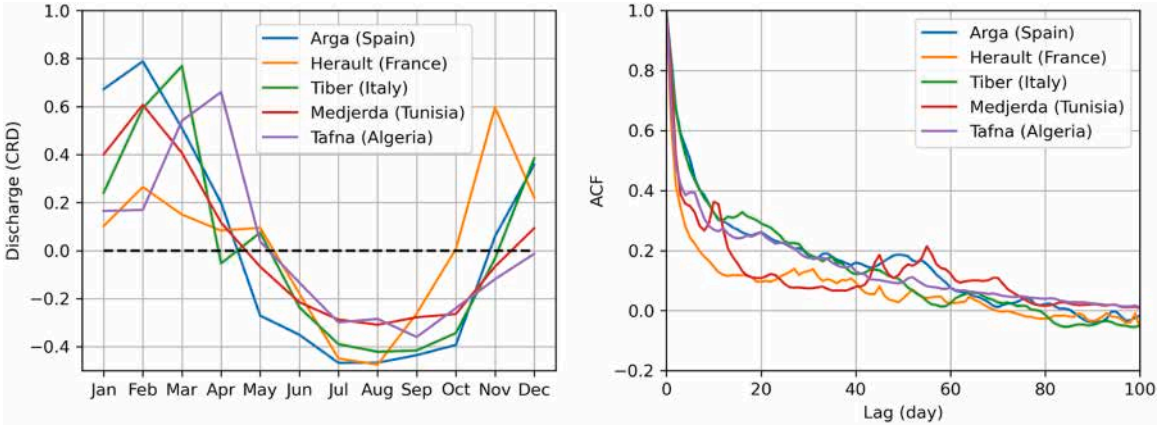

Fig. 4. Basic streamflow time series analysis for the catchment selection: (left) seasonality with centered reduced data (CRD) of the streamflow time series and (right) the auto-correlation function (ACF) computed with the daily streamflow time series.

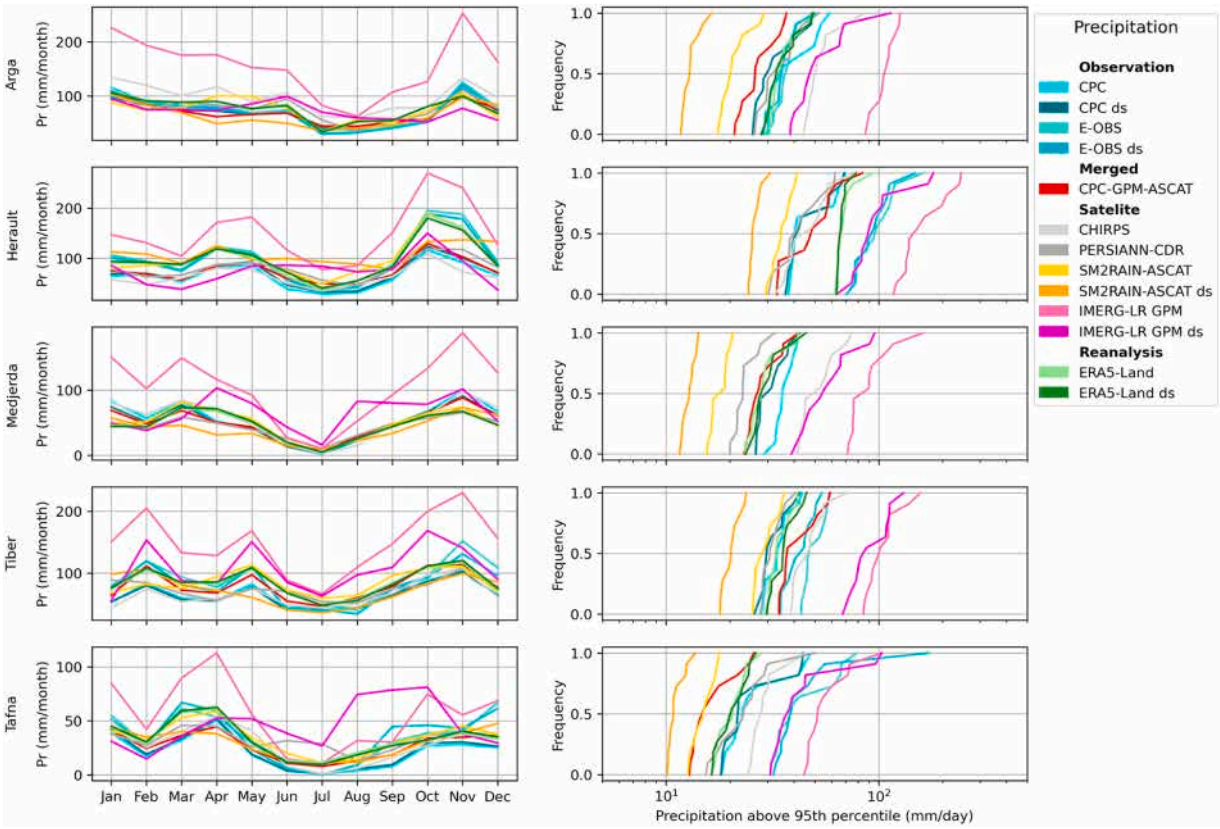

Fig. 5. Analysis of the various precipitation datasets: (left) monthly cumulative precipitation and (right) cumulative probability distribution of the daily precipitation rate above the 95th percentile for the various precipitation datasets for each catchment.

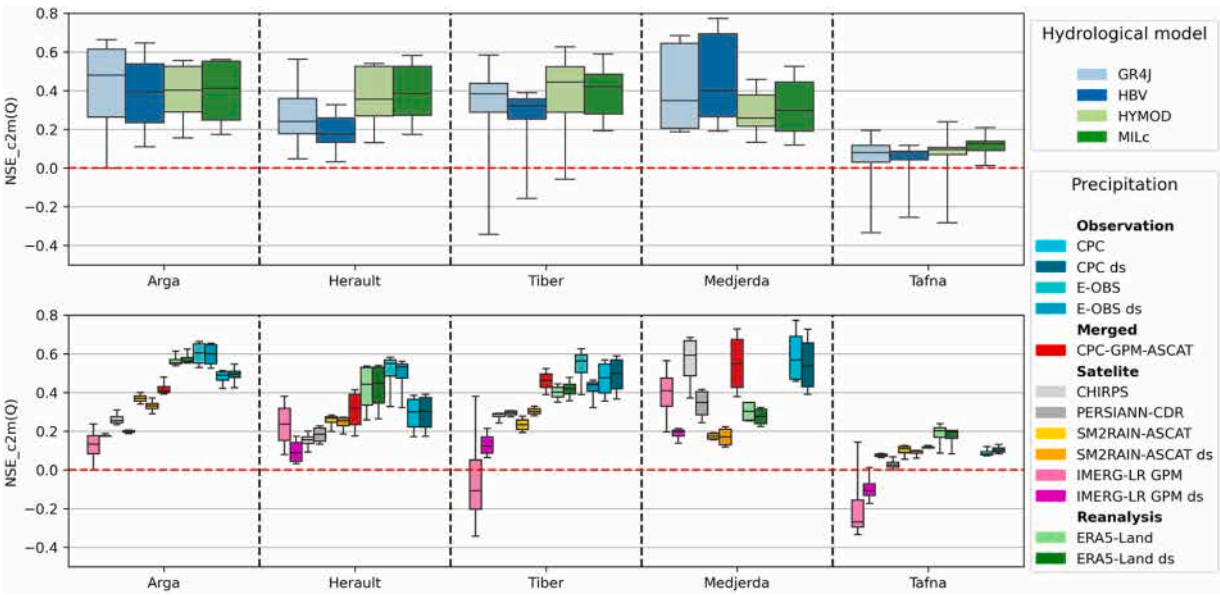

Fig. 6. Boxplot of NSE_c2m computed over the calibration period for each catchment considering (top) various hydrological models (each boxplot includes the thirteen precipitation products) and (bottom) various precipitation datasets (each boxplot includes the four hydrological models). The red dotted line represents NSE_c2m equal to zero.

percentile for Tiber. Then, downscaling IMERG-LR GPM seems to limit the overestimation of precipitation, regarding both precipitation seasonality and high precipitation events. Conversely, SM2RAIN-ASCAT underestimates the daily precipitation above the 95th percentile while the downscaling leads to a more significant underestimation. Also, the downscaling for ERA5-Land, E-OBS and CPC do not affect so much the daily precipitation above the 95th percentile.

4.3. Precipitation versus hydrological model performance

The first evaluation investigates how model performance is affected by the selection of both HM and precipitation datasets. Here, only the streamflow time series are considered as observation to perform the parameter estimation. Fig. 6 shows the boxplots of the model performance depending on the HM (including each of the precipitation datasets) as well as depending on the precipitation dataset (including each of the HM). The various HMs show a certain range of model performance when accounting for uncertainties related to the forcing precipitation datasets as well as parametric uncertainties. Regarding Herault and Tiber, the median of NSE_c2m with both HYMOD and MILc models outperforms GR4J and HBV while the maximum values look pretty close except with HBV showing lower model performance. Regarding Arga and Medjerda, the median of NSE_c2m do not show big difference while GR4J and HBV outperform regarding the maximum NSE_c2m value. Regarding both Tiber and Tafna, the model performance for GR4J, HBV and HYMOD ranges down to negative values (i.e. showing predictive skills lower than the naïve predictor of the NSE criteria) while MILc model generally shows smaller range of performance compared with the other model also avoiding negative NSE_c2m values on each of the five test catchments. One should note the very poor performance for Tafna catchment, likely the most arid one, where daily data is probably not adapted to capture hydrological dynamics. Also, in this mountainous basin with a lot of erosion, the daily discharge data may not be very accurate if the rating curves are not updated regularly (Rachdane et al., 2024).

The model performance using various precipitation datasets ranges from poor NSE_c2m values with IMERG-LR GPM to satisfactorily NSE_c2m values using either ERA5-Land, CPC or E-OBS precipitation datasets. Ranking the various precipitation datasets (Fig. 7) shows that precipitation datasets derived from observations (i.e., CPC and E-OBS) or reanalysis (ERA5-Land) are ranked first while SPP are generally ranked among the latest precipitations products. The SM2RAIN-ASCAT products generally show the best ranking among the SPP while the aggregated product CPC-GPM-ASCAT shows ranking in between SSP and observations/reanalysis precipitation datasets. The CPC-GPM-ASCAT allows to reach model performance close to observation/reanalysis precipitation datasets (Fig. 6). Indeed, the maximum NSE_c2m value obtained using CPC-GPM-ASCAT outperforms any other SPPs on each of the five test catchments. One should note that for both Tiber and Medjerda rivers the CPC-GPM-ASCAT outperforms ERA5-Land.

4.4. Investigating the multi-scale structure of model errors

The orthogonal wavelet decomposition is performed on both observed and simulated streamflow time series and allows evaluating the correlation across the various temporal scales following a dyadic scale (Fig. 8). As already mentioned, the streamflow prediction using observation precipitation datasets outperforms the streamflow prediction using SPP datasets. Using CPC, E-OBS and ERA5-Land precipitation datasets allow the correlation between observed and simulated streamflow to stay high across temporal scales. Herault and Tiber show pretty similar patterns, with a progressive increase of the correlation when increasing temporal scale. The CPC, E-OBS and ERA5-Land outperform SPP across the temporal scale from 2 days to 16 days while SPPs show lower correlations as well as a very low correlation for the short temporal scales. In accordance with the previous evaluation, CPC-GPM-ASCAT shows correlation in between SPPs and either gauge based or reanalysis derived precipitation products. The correlation across scales shows a pattern close to the one observed with the CPC within every catchment as well as similar pattern with IMERG-GPM LR for every catchment except Tafna. Regarding Tafna, CPC-GPM-ASCAT and CPC show a V-shape curve with a local minimum on 8-days scale while IMERG-GPM LR

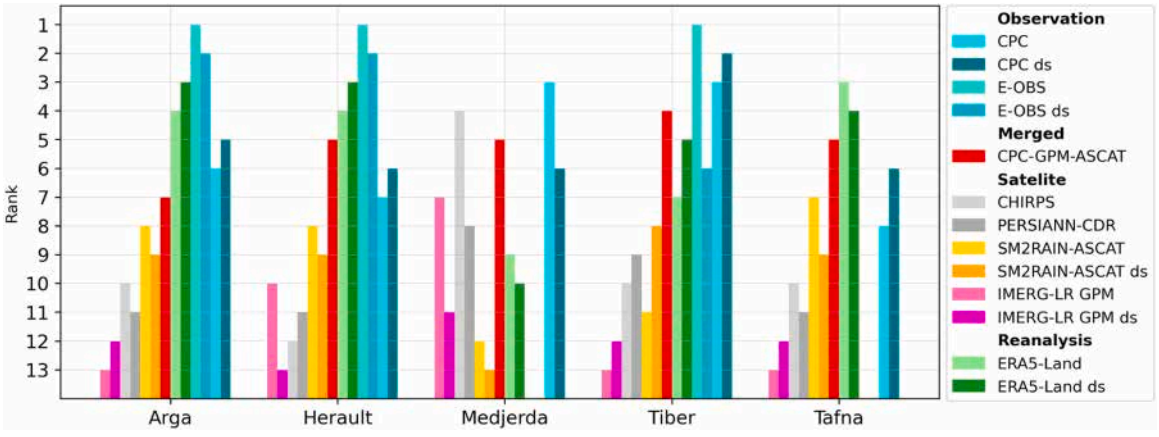

Fig. 7. Ranking of the precipitation datasets evaluated with four HMs. The ranking is derived from the mean NSE_c2m computed with simulated hydrographs by sampling the posterior distribution with the four HMs.

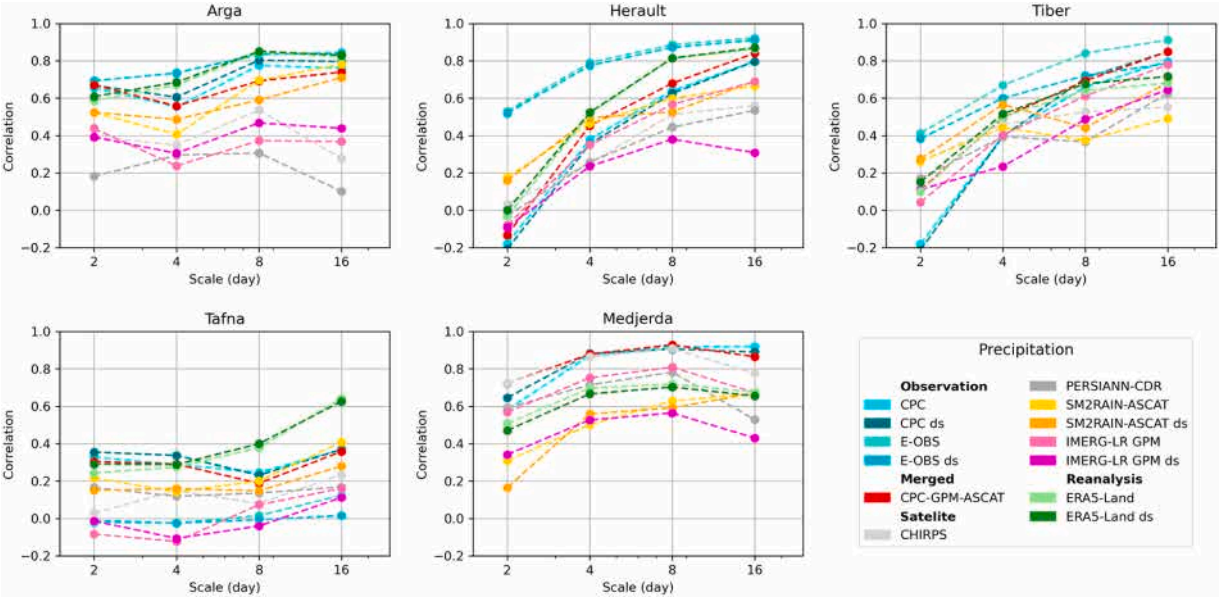

Fig. 8. Decomposition of the model errors across temporal scales based on the orthogonal wavelet decomposition.

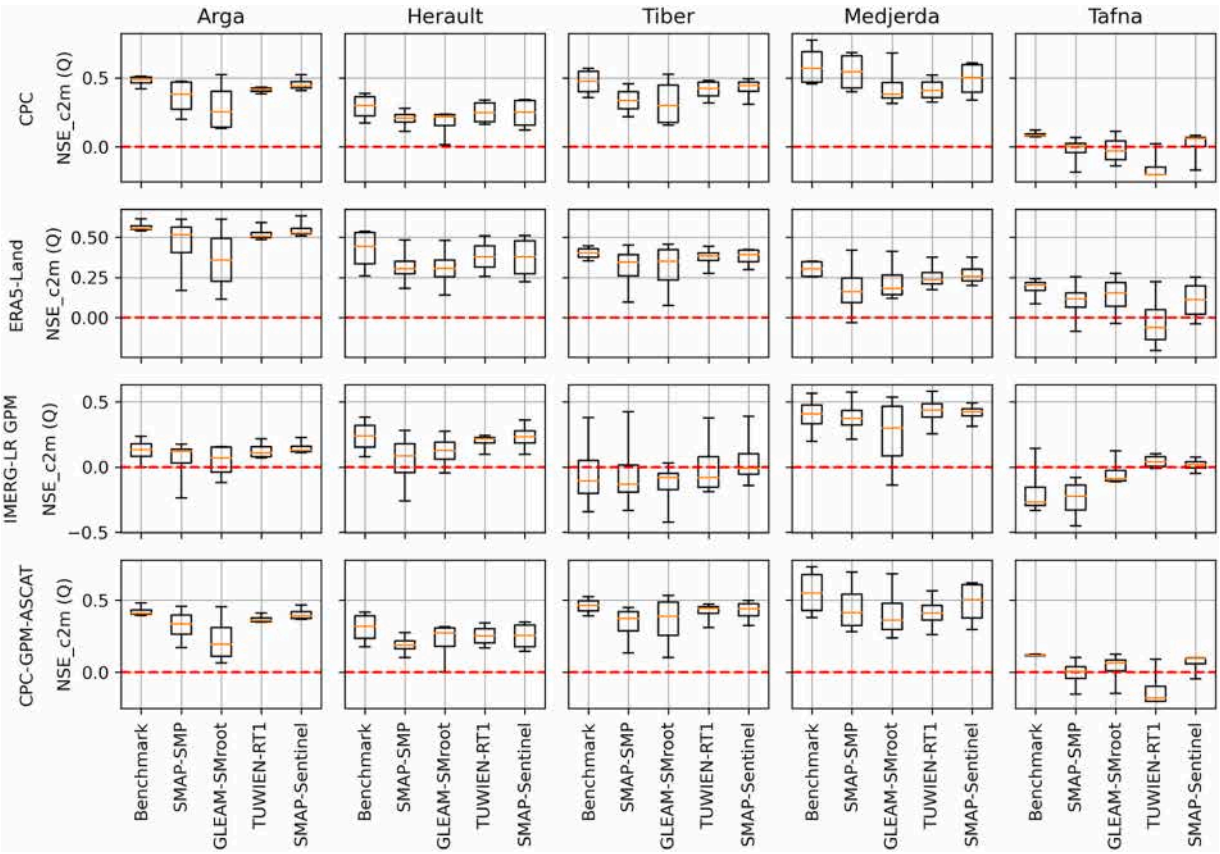

Fig. 9. Boxplot of the NSE_c2m considering various precipitation datasets (CPC, ERA5-Land, IMERG-LR GPM and CPC-GPM-ASCAT) combined with soil moisture accounting with the four products (SMAP-SMP, GLEAM-SMroot, TUWIEN-RT1 and SMAP-Sentinel). The benchmark is computed with the mentioned precipitation products considering the four hydrological models. The benchmark does not consider soil moisture during the parameter estimation procedure.

shows local minimum on 4-days scale. Therefore, the multi-scale structure of model errors for streamflow simulations using CPC-GPM-ASCAT appears to be more related to CPC and SM2RAIN-ASCAT rather than IMERG-LR GPM. While the correlation tends to increase with the increasing temporal scale, the multi-scale structure of model errors over Medjerda river appears stable across the various temporal scales with CPC and CPC-GPM-ASCAT. One should note that CHIRPS outperforms other SPPs for Medjerda and shows performance close to CPC and CPC-GPM-ASCAT.

4.5. Considering soil moisture for hydrological model calibration

To investigate the potential added value of considering soil moisture in hydrological modeling, the parameter estimation is performed (i) considering streamflow time series only (benchmark) and (ii) considering both the streamflow and soil moisture time series taking into account any combination of the eight precipitation and four soil moisture datasets. Fig. 9 shows the box plot of NSE_c2m computed on streamflow when using each of the four soil moisture datasets combined with the following forcing precipitations products: CPC (observation), ERA5-Land (reanalysis), IMERG-LR GPM (satelite) and CPC-GPM-ASCAT (merged). The complete results, including the eight precipitation product is given as supplementary material. Regarding Arga, Herault and Tiber rivers, the results shows that using both SMAP-SMP and GLEAM-SMroot degrades the model performance while using either TUWIEN-RT1 or SMAP-Sentinel shows model performance close to the benchmark. Regarding the Medjerda, using SMAP-SMP and SMAP-Sentinel reach model performance close to the benchmark while using GLEAM-SMroot and TUWIEN-RT1 reach lower model performance. Considering the various test sites as well as considering IMERG-LR GPM precipitation dataset, both TUWIEN-RT1 and SMAP-Sentinel outperforms the model performance when using SMAP-SMP or GLEAM-SMroot. Also, using SMAP-Sentinel combined with IMERG-LR GPM can outperforms benchmark regarding Tiber and Tafna although the IMERG-LR GPM offers poor model performance. In a general way, using TUWIEN-RT1 and SMAP-Sentinel show a lower spread of the model performance in comparison with SMAP-SMP and GLEAM-SMroot. For instance, when using CPC precipitation over Arga, the model performances range from NSE_c2m around 0.1–0.5 when using SMAP-SMP or GLEAM-SMroot, while the model performances range from NSE_c2m around 0.4–0.5 when using TUWIEN-RT1 and GLEAM-SMroot. Nonetheless, TUWIEN-RT1 show a significant decrease of NSE_c2m when combined with either CPC, ERA5-Land and CPC-GPM-ASCAT. Indeed, the benchmark show positive values, around 0.2 but reach negative values when combined with TUWIEN-RT1. Conversely, IMERG-LR GPM show really poor benchmark performance (negative value of NSE_c2m) while it may reach positive value when combined with TUWIEN-RT1, and so appears to compensate the inconsistency of the GPM-IMERG LR precipitation over this catchment. Finally, regarding Arga, Herault, Tiber and Medjerda, the modeling results using Sentinel-1 derived soil moisture appears more consistent with the benchmark regardless the forcing precipitation (either observation, reanalysis, satellite or merged). Conversely, regarding Tafna, the Sentinel-1 derived soil moisture products bring contradictory results where the soil moisture accounting degrades the simulation in case the benchmark brings predictive skills (positive NSE_c2m value) but can improve the simulation when the benchmark is very low.

5. Discussion

In this study, thirteen precipitation products (eight precipitation among which five have been downscaled to 1 km of spatial resolution) and four soil moisture products are combined in a multi-model workflow to investigate the predictive uncertainties in hydrological modeling in the MR. The modeling exercise provides streamflow simulation results considering various source of precipitations (observations, satellite, reanalysis and merged) as well as various satellite soil moisture products. On one hand, the various precipitation datasets are used as forcing data for HMs, while, on the other hand, the various soil moisture datasets are used for HM calibration. The selection of both precipitation and soil moisture datasets for the above-mentioned application constitutes a key point for hydrological modeling since using various datasets leads to significant variability in terms of hydrological model performance. Also, to avoid misinterpretation related to the potential compensation between precipitation and HMs, the present study introduces a multi-model and multi-parameter methodology using a Bayesian inversion framework. Then, the predictive performance can be assessed through a statistical distribution rather than a single optimum (i.e., a single HM with a single set of optimal parameters) and so provide better robustness for the evaluation of the various precipitations and soil moisture datasets. Among a large number of datasets, finding a suitable precipitation dataset for a given application is not straightforward and requires an evaluation exercise. In this study, the evaluation is performed using lumped parameter hydrological modeling for Mediterranean catchments characterized as mesoscale, rainfall-driven, with short response time and typical Mediterranean regime with dryness during the summer period. Nonetheless, the proposed methodology can be easily replicated, providing an ensemble of precipitation and soil moisture products is available. One should mention that using SSPs in hydrological modeling of large scale hydrosystems has been widely done over the past decades. The developments of new high (or hyper) resolution product of the water cycle component will be helpful to envisage applications on small to mesoscale catchments; the latter constitutes one of the challenges for spatial hydrology, with development of dedicated mission for better spatial resolution of observation of surface water bodies (e.g., SWOT mission) and international initiative for a better description of the terrestrial water cycle (Brocca et al., 2024).

The various precipitation datasets are considered as forcing data for hydrological modeling, considering widely used precipitation datasets either observation based (E-OBS, CPC), satellite derived (IMERG-LR GPM, CHIRPS, PERSIANN-CDR, SM2RAIN-ASCAT) or derived from reanalysis (ERA5-Land) and the newly developed aggregated precipitation products CPC-GPM-ASCAT (Filippucci et al., 2023). The results show that E-OBS, CPC and ERA5-Land generally outperform the satellite derived precipitation products, reaching satisfactorily results in terms of model performance. This is not observed within Medjerda river where CHIRPS offers model performance comparable to CPC, with NSE_c2m ranging from 0.4 to 0.8. One should also note that on Medjerda CHIRPS, PERSIANN-CDR and

IMERG-LR GPM outperform ERA5-Land that gives NSE_c2m around 0.5. The evaluation of precipitation products based on hydrological modeling shows that the CPC-GPM-ASCAT precipitation products is mostly ranked in between satellite derived precipitation and either gauge based or reanalysis precipitation products.

The results show that downscaling precipitation products from native resolution to 1 km of spatial resolution does not significantly affect the lumped parameter hydrological model performance when considering E-OBS, CPC, ERA5-Land and SM2RAIN-ASCAT. Conversely, downscaling IMERG-LR GPM affects the model performance in a positive way for Arga, Tiber and Tafna while it affects in a negative way for Herault and Medjerda. One should note that downscaling brings better results over test sites in which the original IMERG-LR GPM precipitation brings poor simulations results, with negative NSE_c2m values. Therefore, downscaling precipitation product for lumped parameter hydrological modeling appears not improving streamflow simulation results overs the five test sites. Nonetheless, the merged CPC-GPM-ASCAT product (merging downscaled CPC, IMERG-LR GPM and SM2RAIN-ASCAT) may outperforms ERA5-Land precipitation (Tiber and Medjerda) and still outperforms satellite precipitation products (both original and downscaled).

Investigating the multi-scale structure of model errors accounting for the various precipitation products helps to better capture how the aggregated product CPC-GPM-ASCAT includes the informative content of every single CPC, IMERG-LR GPM and SM2RAIN-ASCAT precipitation products. Such an analysis allows a deeper understanding of how hydrological modeling may benefit from aggregated precipitation products. Herault, give a pretty clear example for the distribution of informative content of precipitation products across temporal scales, ranging from poor predictive skills among 2-days scale (correlation close to 0 with IMERG-LR GPM) to high predictive skills among the 16-days scale in between SM2RAIN-ASCAT and CPC (with correlation around 0.8), while IMERG-LR GPM shows significantly lower predictive skills among the 16-days scale (with correlation around 0.3). Then, such an assessment of multi-scale hydrological model errors forced with various precipitation products as well as merged precipitation products may help to better investigate how the merged products may include the informative content of precipitation and their influence on streamflow simulation.

Also, considering soil moisture within the parameter estimation procedure has shown great interest in reducing the range of predictive uncertainties even if the overall model performance over streamflow time series can be a little decreased (due to pareto optimality between model performance on streamflow and soil moisture time series). Then, in most cases, using Sentinel-1 derived soil moisture products (i.e., TUWIEN-RT1 and SMAP-Sentinel) shows predictive performance close to the benchmark and shows a significantly decreased spread of the model performance on streamflow time series. The conclusion about using Sentinel-1 derived soil moisture relies here on using various source of precipitation products, various lumped parameters HM accounting for both structural and parametric uncertainties. Results shows promising perspectives for using Sentinel-1 derived soil moisture in hydrological modeling. In this study, the comparison with SMAP-SMP and GLEAM-SMroot have evidenced discrepancies between the temporal variability of soil moisture and the saturation of the soil moisture store, while both products offers daily temporal resolution with a coarser spatial resolution compared with Sentinel-1 derived soil moisture. Then, despite discontinuous daily chronicles using Sentinel-1 derived soil moisture appears more consistent with the saturation of soil moisture store of four hydrological models. This might testify of the advantages of a higher spatial resolution against temporal resolution. Nonetheless, Sentinel-1 derived soil moisture limitation has been identified for application over semi-arid area and so negatively impacts the streamflow simulation for Tafna catchment.

6. Conclusion

While large-scale hydrology largely benefited from EO systems development in the past decades, the small and mesoscale applications did not take advantage of it due to the coarse resolution of satellite-derived estimation of the various components of the continental water cycle. In this study, the results showed that lumped parameter hydrological modeling over mesoscale catchments in the Mediterranean region can take advantages of Sentinel-1 derived soil moisture (spatial resolution of 1 km). Conversely, downscaling precipitation products to 1 km of spatial resolution do not impact significantly the streamflow simulation compared with original precipitation products. However, the merged CPC-GPM-ASCAT product (spatial resolution of 1 km) outperforms SPPs (CHIRPS, PERSIANN-CDR, SM2RAIN-ASCAT and IMERG-LR GPM) and may outperforms ERA5-Land reanalysis in some cases. More investigations are required to assess to which extent hydrological modeling over small and mesoscale hydro(geo)logical systems can benefit from high-resolution products of the various components of the continental water cycle. The present study assessed some high-resolution precipitation and soil moisture products in comparison with widely used products at a coarser spatial resolution and do not consider uncertainties related to evapotranspiration. Such a methodology might be applied to assess the potential added value of high resolution of evapotranspiration products that will developed in the coming years (e.g., TRISHNA mission Lagouarde et al., 2018 and SBG mission Cawse-Nicholson et al., 2021).

The proposed methodology opens interesting perspectives for various applications in hydrology. It allows investigating how HMs may compensate for bias in forcing data (i.e., precipitation and evapotranspiration) as well as identifying an optimal combination of HM and SPP for streamflow predictions over a sample of gauged catchments. The combination of streamflow predictions relying on several HMs and SPPs may help to provide more reliable streamflow prediction over ungauged catchments and a deeper assessment of hydrological model uncertainties. Such a methodology might be developed for uncertainties attribution in hydrological modeling chains, allowing a better evaluation of model performance on streamflow as well as a better assessment of predictive uncertainty. This constitutes a key challenge for prospective exercise under both anthropogenic and climate change impacts, where using robust hydrological modeling chains is required to ensure the reliability of streamflow simulation with changing environment.

Data access

This work used the data collected in the framework of the 4DMED-hydrology project: https://www.4dmed-hydrology.org/. The data are freely available: https://edp-portal.eurac.edu/cdb_doc/4dmed/

CRediT authorship contribution statement

Yves Tramblay: Writing – original draft, Methodology. **Christian Massari:** Writing – review & editing, Project administration, Methodology. **Paolo Filippucci:** Writing – review & editing, Data curation, Conceptualization. **Pere Quintana-Seguí:** Writing – review & editing. **Hamouda Dakhlaoui:** Writing – review & editing. **Hamouda Boutaghane:** Writing – review & editing. **Roger Clavera-Gispert:** Writing – review & editing. **Raphael Quast:** Writing – review & editing, Data curation. **Tayeb Boulmaiz:** Writing – review & editing. **Vianney Sivelle:** Writing – original draft, Software, Methodology, Conceptualization. **Mariette Vreugdenhill:** Writing – review & editing, Data curation.

Declaration of Competing Interest

The authors declare that they have no known competing financial interests or personal relationships that could have appeared to influence the work reported in this paper

Acknowledgements

This work benefit from financial support by the European Space Agency (ESA) with the 4DMED-hydrology project (ESA contract n. 4000136272/21/I-EF) and from the Italian National Research Council (CNR) through a senior research grant (n. IRPI 001 2023 PG) attributed to V. Sivelle for a post-doctoral position at the Research Institute for Geo-Hydrological Protection (IRPI).

Appendix A. Supporting information

Supplementary data associated with this article can be found in the online version at doi:10.1016/j.ejrh.2025.103015.

Data availability

Data will be made available on request.

References

Alfieri, L., Avanzi, F., Delogu, F., Gabellani, S., Bruno, G., Campo, L., Libertino, A., Massari, C., Tarpanelli, A., Rains, D., Miralles, D.G., Quast, R., Vreugdenhil, M., Wu, H., Brocca, L., 2022. High-resolution satellite products improve hydrological modeling in northern Italy. Hydrol. Earth Syst. Sci. 26, 3921–3939. https://doi.org/10.5194/hess-26-3921-2022.

Al-Khoury, I., Boithias, L., Sivelle, V., Bailey, R.T., Abbas, S.A., Filippucci, P., Massari, C., Labat, D., 2024. Evaluation of precipitation products for small karst catchment hydrological modeling in data-scarce mountainous regions. J. Hydrol. 645, 132131. https://doi.org/10.1016/j.jhydrol.2024.132131.

Andréassian, V., 2023. On the (im)possible validation of hydrogeological models. Comptes Rendus. Géoscience 355, 1–9. https://doi.org/10.5802/crgeos.142.

Arsenault, R., Brissette, F., Martel, J.-L., 2018. The hazards of split-sample validation in hydrological model calibration. J. Hydrol. 566, 346–362. https://doi.org/10.1016/j.jhydrol.2018.09.027.

Ashouri, H., Hsu, K.-L., Sorooshian, S., Braithwaite, D.K., Knapp, K.R., Cecil, L.D., Nelson, B.R., Prat, O.P., 2015. PERSIANN-CDR: daily precipitation climate data record from multisatellite observations for hydrological and climate studies. Bull. Am. Meteorol. Soc. 96, 69–83. https://doi.org/10.1175/BAMS-D-13-00068.1.

Bargaoui, Z., Dakhlaoui, H., Houcine, A., 2008. Modélisation pluie-débit et classification hydroclimatique. rseau 21, 233–245. https://doi.org/10.7202/018468ar.

Bechtold, M., Modanesi, S., Lievens, H., Baguis, P., Brangers, I., Carrassi, A., Getirana, A., Gruber, A., Heyvaert, Z., Massari, C., Scherrer, S., Vannitsem, S., Lannoy, G. D., 2023. Assimilation of Sentinel-1 backscatter into a land surface model with river routing and its impact on streamflow simulations in two belgian catchments. J. Hydrometeorol. 24, 2389–2408. https://doi.org/10.1175/JHM-D-22-0198.1.

Bennett, N.D., Croke, B.F.W., Guariso, G., Guillaume, J.H.A., Hamilton, S.H., Jakeman, A.J., Marsili-Libelli, S., Newham, L.T.H., Norton, J.P., Perrin, C., Pierce, S.A., Robson, B., Seppelt, R., Voinov, A.A., Fath, B.D., Andreassian, V., 2013. Characterising performance of environmental models. Environ. Model. Softw. 40, 1–20. https://doi.org/10.1016/j.envsoft.2012.09.011.

Bergström, S., 1992. The HBV model - its structure and applications.

Beven, K., 2001. On explanatory depth and predictive power. Hydrol. Process. 15, 3069–3072. https://doi.org/10.1002/hyp.500.

Bolten, J.D., Crow, W.T., Zhan, X., Jackson, T.J., Reynolds, C.A., 2010. Evaluating the utility of remotely sensed soil moisture retrievals for operational agricultural drought monitoring. IEEE J. Sel. Top. Appl. Earth Obs. Remote Sens. 3, 57–66. https://doi.org/10.1109/JSTARS.2009.2037163.

Box, G.E., Jenkins, G.M., Reinsel, G.C., Ljung, G.M., 2008. Time series analysis: Forecasting and control. John Wiley&Sons Inc. ed, Hoboken.

Boyle, D.P., Gupta, H.V., Sorooshian, S., 2003. Multicriteria calibration of hydrologic models. In: Duan, Q., Gupta, H.V., Sorooshian, S., Rousseau, A.N., Turcotte, R. (Eds.), Water Science and Application. American Geophysical Union, Washington, D. C., pp. 185–196. https://doi.org/10.1029/WS006p0185

Brocca, L., Barbetta, S., Camici, S., Ciabatta, L., Dari, J., Filippucci, P., Massari, C., Modanesi, S., Tarpanelli, A., Bonaccorsi, B., Mosaffa, H., Wagner, W., Vreugdenhil, M., Quast, R., Alfieri, L., Gabellani, S., Avanzi, F., Rains, D., Miralles, D.G., Mantovani, S., Briese, C., Domeneghetti, A., Jacob, A., Castelli, M., Camps-Valls, G., Volden, E., Fernandez, D., 2024. A Digital Twin of the terrestrial water cycle: a glimpse into the future through high-resolution Earth observations. Front. Sci. 1. https://doi.org/10.3389/fsci.2023.1190191.

Brocca, L., Ciabatta, L., Massari, C., Moramarco, T., Hahn, S., Hasenauer, S., Kidd, R., Dorigo, W., Wagner, W., Levizzani, V., 2014. Soil as a natural rain gauge: estimating global rainfall from satellite soil moisture data. J. Geophys. Res. Atmos. 119, 5128–5141. https://doi.org/10.1002/2014JD021489.

Brocca, L., Filippucci, P., Hahn, S., Ciabatta, L., Massari, C., Camici, S., Schüller, L., Bojkov, B., Wagner, W., 2019. SM2RAIN–ASCAT (2007–2018): global daily satellite rainfall data from ASCAT soil moisture observations. Earth Syst. Sci. Data 11, 1583–1601. https://doi.org/10.5194/essd-11-1583-2019.

Brocca, L., Melone, F., Moramarco, T., 2011. Distributed rainfall-runoff modelling for flood frequency estimation and flood forecasting. Hydrol. Process. 25, 2801–2813. https://doi.org/10.1002/hyp.8042.

Camici, S., Ciabatta, L., Massari, C., Brocca, L., 2018. How reliable are satellite precipitation estimates for driving hydrological models: a verification study over the Mediterranean area. J. Hydrol. 563, 950–961. https://doi.org/10.1016/j.jhydrol.2018.06.067.

Camici, S., Giuliani, G., Brocca, L., Massari, C., Tarpanelli, A., Farahani, H.H., Sneeuw, N., Restano, M., Benveniste, J., 2022. Synergy between satellite observations of soil moisture and water storage anomalies for runoff estimation. Geosci. Model Dev. 15, 6935–6956. https://doi.org/10.5194/gmd-15-6935-2022.

Cantoni, E., Tramblay, Y., Grimaldi, S., Salamon, P., Dakhlaoui, H., Dezetter, A., Thiemig, V., 2022. Hydrological performance of the ERA5 reanalysis for flood modeling in Tunisia with the LISFLOOD and GR4J models. J. Hydrol. Reg. Stud. 42, 101169. https://doi.org/10.1016/j.ejrh.2022.101169.

Cawse-Nicholson, K., Townsend, P.A., Schimel, D., Assiri, A.M., Blake, P.L., Buongiorno, M.F., Campbell, P., Carmon, N., Casey, K.A., Correa-Pabón, R.E., Dahlin, K. M., Dashti, H., Dennison, P.E., Dierssen, H., Erickson, A., Fisher, J.B., Frouin, R., Gatebe, C.K., Gholizadeh, H., Gierach, M., Glenn, N.F., Goodman, J.A., Griffith, D.M., Guild, L., Hakkenberg, C.R., Hochberg, E.J., Holmes, T.R.H., Hu, C., Hulley, G., Huemmrich, K.F., Kudela, R.M., Kokaly, R.F., Lee, C.M., Martin, R., Miller, C.E., Moses, W.J., Muller-Karger, F.E., Ortiz, J.D., Otis, D.B., Pahlevan, N., Painter, T.H., Pavlick, R., Poulter, B., Qi, Y., Realmuto, V.J., Roberts, D., Schaepman, M.E., Schneider, F.D., Schwandner, F.M., Serbin, S.P., Shiklomanov, A.N., Stavros, E.N., Thompson, D.R., Torres-Perez, J.L., Turpie, K.R., Tzortziou, M., Ustin, S., Yu, Q., Yusup, Y., Zhang, Q., 2021. NASA's surface biology and geology designated observable: a perspective on surface imaging algorithms. Remote Sens. Environ. 257, 112349. https://doi.org/10.1016/j.rse.2021.112349.

Cenci, L., Pulvirenti, L., Boni, G., Chini, M., Matgen, P., Gabellani, S., Squicciarino, G., Pierdicca, N., 2017. An evaluation of the potential of Sentinel 1 for improving flash flood predictions via soil moisture–data assimilation. Adv. Geosci. 44, 89–100. https://doi.org/10.5194/adgeo-44-89-2017.

Chen, M., Shi, W., Xie, P., Silva, V.B.S., Kousky, V.E., Wayne Higgins, R., Janowiak, J.E., 2008. Assessing objective techniques for gauge-based analyses of global daily precipitation. D04110 J. Geophys. Res. (Atmospheres) 113. https://doi.org/10.1029/2007JD009132.

Ciabatta, L., Brocca, L., Massari, C., Moramarco, T., Gabellani, S., Puca, S., Wagner, W., 2016. Rainfall-runoff modelling by using SM2RAIN-derived and state-of-the-art satellite rainfall products over Italy. Int. J. Appl. Earth Obs. Geoinf. Adv. Valid. Appl. Remote. Sense Soil Moisture Part 2 48, 163–173. https://doi.org/10.1016/j.jag.2015.10.004.

Cornes, R.C., van der Schrier, G., van den Besselaar, E.J.M., Jones, P.D., 2018. An ensemble version of the E-OBS temperature and precipitation data sets. J. Geophys. Res. Atmospheres 123, 9391–9409. https://doi.org/10.1029/2017JD028200.

Cousquer, Y., Jourde, H., 2022. Reducing uncertainty of karst aquifer modeling with complementary hydrological observations for the sustainable management of groundwater resources. J. Hydrol., 128130 https://doi.org/10.1016/j.jhydrol.2022.128130.

Das, N.N., Entekhabi, D., Dunbar, R.S., Chaubell, M.J., Colliander, A., Yueh, S., Jagdhuber, T., Chen, F., Crow, W., O'Neill, P.E., Walker, J.P., Berg, A., Bosch, D.D., Caldwell, T., Cosh, M.H., Collins, C.H., Lopez-Baeza, E., Thibeault, M., 2019. The SMAP and Copernicus Sentinel 1A/B microwave active-passive high resolution surface soil moisture product. Remote Sens. Environ. 233, 111380. https://doi.org/10.1016/j.rse.2019.111380.

Eini, M.R., Massari, C., Piniewski, M., 2023. Satellite-based soil moisture enhances the reliability of agro-hydrological modeling in large transboundary river basins. Sci. Total Environ. 873, 162396. https://doi.org/10.1016/j.scitotenv.2023.162396.

Entekhabi, D., Njoku, E.G., O'Neill, P.E., Kellogg, K.H., Crow, W.T., Edelstein, W.N., Entin, J.K., Goodman, S.D., Jackson, T.J., Johnson, J., Kimball, J., Piepmeier, J. R., Koster, R.D., Martin, N., McDonald, K.C., Moghaddam, M., Moran, S., Reichle, R., Shi, J.C., Spencer, M.W., Thurman, S.W., Tsang, L., Van Zyl, J., 2010. The soil moisture active passive (SMAP) mission. Proc. IEEE 98, 704–716. https://doi.org/10.1109/JPROC.2010.2043918.

Feldman, A.F., Short Gianotti, D.J., Dong, J., Akbar, R., Crow, W.T., McColl, K.A., Konings, A.G., Nippert, J.B., Tumber-Dávila, S.J., Holbrook, N.M., Rockwell, F.E., Scott, R.L., Reichle, R.H., Chatterjee, A., Joiner, J., Poulter, B., Entekhabi, D., 2023. Remotely sensed soil moisture can capture dynamics relevant to plant water uptake. Water Resour. Res. 59, e2022WR033814. https://doi.org/10.1029/2022WR033814.

Ferreira, P.M., de, L., Paz, A.R., da, Bravo, J.M., 2020. Objective functions used as performance metrics for hydrological models: state-of-the-art and critical analysis. RBRH 25, e42. https://doi.org/10.1590/2318-0331.252020190155.

Filippucci, P., Brocca, L., Ciabatta, L., Mosaffa, H., Avanzi, F., Massari, C., 2025. Development of HYPER-P: HYdroclimatic PERformance-enhanced precipitation at 1 km/daily over the Europe-Mediterranean region from 2007 to 2022. Earth Syst. Sci. Data Discuss. 1–55. https://doi.org/10.5194/essd-2025-156.

Filippucci, P., Brocca, L., Quast, R., Ciabatta, L., Saltalippi, C., Wagner, W., Tarpanelli, A., 2022. High-resolution (1km) satellite rainfall estimation from SM2RAIN applied to Sentinel-1: Po river basin as a case study. Hydrol. Earth Syst. Sci. 26, 2481–2497. https://doi.org/10.5194/hess-26-2481-2022.

Filippucci, P., Ciabatta, L., Mosaffa, H., Brocca, L., 2024. Improving the resolution of satellite precipitation products in Europe. https://doi.org/10.5194/egusphere-egu24-16956.

Filippucci, P., Mosaffa, H., Avanzi, F., Brocca, L., Massari, C., 2023. 4DMED precipitation product: 1 km merged precipitation from CPC, GPM and SM2RAIN-ASCAT for mediterranean basin. https://doi.org/10.5281/zenodo.10402392.

Flinck, A., Folton, N., Arnaud, P., 2021. Assimilation of Piezometric Data to Calibrate Parsimonious Daily Hydrological Models. Water 13, 2342. https://doi.org/10.3390/w13172342.

Freedman, D., Pisani, R., Purves, R., Adhikari, A., 2007. Statistics. WW Norton & Company, New York.

Funk, C., Peterson, P., Landsfeld, M., Pedreros, D., Verdin, J., Shukla, S., Husak, G., Rowland, J., Harrison, L., Hoell, A., Michaelsen, J., 2015. The climate hazards infrared precipitation with stations—a new environmental record for monitoring extremes. Sci. Data 2, 150066. https://doi.org/10.1038/sdata.2015.66.

Gauch, M., Kratzert, F., Gilon, O., Gupta, H., Mai, J., Nearing, G., Tolson, B., Hochreiter, S., Klotz, D., 2022. Def. Metr. Metr. Sufficiently Encode Typ. Hum. Prefer. Hydrol. Model Perform.

Gupta, A., Govindaraju, R.S., 2019. Propagation of structural uncertainty in watershed hydrologic models. J. Hydrol. 575, 66–81. https://doi.org/10.1016/j.jhydrol.2019.05.026.

Hargreaves, G.H., Samani, Z.A., 1982. Estimating potential evapotranspiration. J. Irrig. Drain. Div. 108, 225–230. https://doi.org/10.1061/JRCEA4.0001390.

Hastings, W.K., 1970. Monte Carlo sampling methods using markov chains and their applications. Biometrika 57, 97–109. https://doi.org/10.2307/2334940.

Hauduc, H., Neumann, M.B., Muschalla, D., Gamerith, V., Gillot, S., Vanrolleghem, P.A., 2015. Efficiency criteria for environmental model quality assessment: a review and its application to wastewater treatment. Environ. Model. Softw. 68, 196–204. https://doi.org/10.1016/j.envsoft.2015.02.004.

Herrera, P.A., Marazuela, M.A., Hofmann, T., 2022. Parameter estimation and uncertainty analysis in hydrological modeling. WIREs Water 9, e1569. https://doi.org/10.1002/wat2.1569.

Huffman, G.J., Bolvin, D.T., Nelkin, E.J., Tan, J., 2019. Integrated Multi-satellitE Retrievals for GPM (IMERG) technical documentation (No. Nasa/Gsfc Code, 612 (47)).

Huo, J., Liu, L., 2020. Evaluation method of multiobjective functions' combination and its application in hydrological model evaluation. Comput. Intell. Neurosci. 2020, 8594727. https://doi.org/10.1155/2020/8594727.

Jackson, E.K., Roberts, W., Nelsen, B., Williams, G.P., Nelson, E.J., Ames, D.P., 2019. Introductory overview: Error metrics for hydrologic modelling – a review of common practices and an open source library to facilitate use and adoption. Environ. Model. Softw. 119, 32–48. https://doi.org/10.1016/j.envsoft.2019.05.001.

Karger, D.N., Wilson, A.M., Mahony, C., Zimmermann, N.E., Jetz, W., 2021. Global daily 1 km land surface precipitation based on cloud cover-informed downscaling. Sci. Data 8, 307. https://doi.org/10.1038/s41597-021-01084-6.

Klemeš, V., 1986. Operational testing of hydrological simulation models. Hydrol. Sci. J. 31, 13–24. https://doi.org/10.1080/02626668609491024.

Knoben, W.J.M., Freer, J.E., Peel, M.C., Fowler, K.J.A., Woods, R.A., 2020. A brief analysis of conceptual model structure uncertainty using 36 models and 559 catchments. Water Resour. Res. 56, e2019WR025975. https://doi.org/10.1029/2019WR025975.

Koren, V., Moreda, F., Smith, M., 2008. Use of soil moisture observations to improve parameter consistency in watershed calibration. Phys. Chem. Earth Parts A/B/C. Calibration Process Underst. RainfallRunoff Model. 33, 1068–1080. https://doi.org/10.1016/j.pce.2008.01.003.

Labat, D., Ababou, R., Mangin, A., 2000. Rainfall–runoff relations for karstic springs. Part II: continuous wavelet and discrete orthogonal multiresolution analyses. J. Hydrol. 238, 149–178. https://doi.org/10.1016/S0022-1694(00)00322-X.

Lagouarde, J.-P., Bhattacharya, B.K., Crébassol, P., Gamet, P., Babu, S.S., Boulet, G., Briottet, X., Buddhiraju, K.M., Cherchali, S., Dadou, I., Dedieu, G., Gouhier, M., Hagolle, O., Irvine, M., Jacob, F., Kumar, A., Kumar, K.K., Laignel, B., Mallick, K., Murthy, C.S., Olioso, A., Ottlé, C., Pandya, M.R., Raju, P.V., Roujean, J.-L., Sekhar, M., Shukla, M.V., Singh, S.K., Sobrino, J., Ramakrishnan, R., 2018. The Indian-French Trishna Mission: Earth Observation in the Thermal Infrared with High Spatio-Temporal Resolution, in: IGARSS 2018 - 2018 IEEE International Geoscience and Remote Sensing Symposium. Presented at the IGARSS 2018 - 2018 IEEE International Geoscience and Remote Sensing Symposium, pp. 4078–4081. https://doi.org/10.1109/IGARSS.2018.8518720.

Lamb, R., Beven, K., Myrabø, S., 1998. Use of spatially distributed water table observations to constrain uncertainty in a rainfall-runoff model. Adv. Water Resour. 22, 305–317. https://doi.org/10.1016/S0309-1708(98)00020-7.

Madelon, R., Rodríguez-Fernández, N.J., Bazzi, H., Baghdadi, N., Albergel, C., Dorigo, W., Zribi, M., 2023. Soil moisture estimates at 1km resolution making a synergistic use of Sentinel data. Hydrol. Earth Syst. Sci. 27, 1221–1242. https://doi.org/10.5194/hess-27-1221-2023.

Maggioni, V., Massari, C., 2018. On the performance of satellite precipitation products in riverine flood modeling: a review. J. Hydrol. 558, 214–224. https://doi.org/10.1016/j.jhydrol.2018.01.039.

Mallat, S.G., 1989. A theory for multiresolution signal decomposition: the wavelet representation. IEEE Trans. Pattern Anal. Mach. Intell. 11, 674–693.

Manoj J, A., Pérez Ciria, T., Chiogna, G., Salzmann, N., Agarwal, A., 2023. Characterising the coincidence of soil moisture – precipitation extremes as a possible precursor to European floods. J. Hydrol. 620, 129445. https://doi.org/10.1016/j.jhydrol.2023.129445.

Massari, C., Brocca, L., Ciabatta, L., Moramarco, T., Gabellani, S., Albergel, C., De Rosnay, P., Puca, S., Wagner, W., 2015. The use of H-SAF soil moisture products for operational hydrology: flood modelling over Italy. Hydrology 2, 2–22. https://doi.org/10.3390/hydrology2010002.

Massari, C., Camici, S., Ciabatta, L., Brocca, L., 2018. Exploiting satellite-based surface soil moisture for flood forecasting in the mediterranean area: state update versus rainfall correction. Remote Sens. 10, 292. https://doi.org/10.3390/rs10020292.

Massari, C., Pellet, V., Tramblay, Y., Crow, W.T., Gründemann, G.J., Hascoetf, T., Penna, D., Modanesi, S., Brocca, L., Camici, S., Marra, F., 2023. On the relation between antecedent basin conditions and runoff coefficient for European floods. J. Hydrol., 130012 https://doi.org/10.1016/j.jhydrol.2023.130012.

Mathevet, T., Michel, C., Andréassian, V., Perrin, C., 2006. A Bound. Version NashSutcliffe Criterion Better Model Assess. Large sets Basins 9.

Mazzilli, N., Guinot, V., Jourde, H., 2012. Sensitivity analysis of conceptual model calibration to initialisation bias. Application to karst spring discharge models. Adv. Water Resour. 42, 1–16. https://doi.org/10.1016/j.advwatres.2012.03.020.

McMillan, H., Araki, R., Gnann, S., Woods, R., Wagener, T., 2023. How do hydrologists perceive watersheds? A survey and analysis of perceptual model figures for experimental watersheds. Hydrol. Process. 37, e14845. https://doi.org/10.1002/hyp.14845.

Merheb, M., Moussa, R., Abdallah, C., Colin, F., Perrin, C., Baghdadi, N., 2016. Hydrological response characteristics of Mediterranean catchments at different time scales: a meta-analysis. Hydrol. Sci. J. 61, 2520–2539. https://doi.org/10.1080/02626667.2016.1140174.

Miralles, D.G., Holmes, T.R.H., De Jeu, R. a M., Gash, J.H., Meesters, A.G.C.A., Dolman, A.J., 2011. Global land-surface evaporation estimated from satellite-based observations. Hydrol. Earth Syst. Sci. 15, 453–469. https://doi.org/10.5194/hess-15-453-2011.

Mladenova, I.E., Bolten, J.D., Crow, W.T., Anderson, M.C., Hain, C.R., Johnson, D.M., Mueller, R., 2017. Intercomparison of soil moisture, evaporative stress, and vegetation indices for estimating corn and soybean yields over the U.S. IEEE J. Sel. Top. Appl. Earth Obs. Remote Sens. 10, 1328–1343. https://doi.org/10.1109/JSTARS.2016.2639338.

Molero, B., Leroux, D.J., Richaume, P., Kerr, Y.H., Merlin, O., Cosh, M.H., Bindlish, R., 2018. Multi-timescale analysis of the spatial representativeness of in situ soil moisture data within satellite footprints. J. Geophys. Res. Atmos. 123, 3–21. https://doi.org/10.1002/2017JD027478.

Monteil, C., Zaoui, F., Le Moine, N., Hendrickx, F., 2020. Multi-objective calibration by combination of stochastic and gradient-like parameter generation rules – the caRamel algorithm. Hydrol. Earth Syst. Sci. 24, 3189–3209. https://doi.org/10.5194/hess-24-3189-2020.

Moore, R.J., 1985. The probability-distributed principle and runoff production at point and basin scales. Hydrol. Sci. J. 30, 273–297. https://doi.org/10.1080/02626668509490989.

Nash, J.E., Sutcliffe, J.V., 1970. River flow forecasting through conceptual models part I — a discussion of principles. J. Hydrol. 10, 282–290. https://doi.org/10.1016/0022-1694(70)90255-6.

Nikolopoulos, E.I., Anagnostou, E.N., Borga, M., 2013. Using high-resolution satellite rainfall products to simulate a major flash flood event in Northern Italy. J. Hydrometeorol. 14, 171–185. https://doi.org/10.1175/JHM-D-12-09.1.

Oudin, L., Perrin, C., Mathevet, T., Andréassian, V., Michel, C., 2006. Impact of biased and randomly corrupted inputs on the efficiency and the parameters of watershed models. J. Hydrol. 320, 62–83. https://doi.org/10.1016/j.jhydrol.2005.07.016.

Perrin, C., Michel, C., Andréassian, V., 2003. Improvement of a parsimonious model for streamflow simulation. J. Hydrol. 279, 275–289. https://doi.org/10.1016/S0022-1694(03)00225-7.

Quan, Z., Teng, J., Sun, W., Cheng, T., Zhang, J., 2015. Evaluation of the HYMOD model for rainfall–runoff simulation using the GLUE method. Proc. IAHS 368, 180–185. https://doi.org/10.5194/piahs-368-180-2015.

Quast, R., Albergel, C., Calvet, J.-C., Wagner, W., 2019. A generic first-order radiative transfer modelling approach for the inversion of soil and vegetation parameters from scatterometer observations. Remote Sens. 11, 285. https://doi.org/10.3390/rs11030285.

Quast, R., Wagner, W., Bauer-Marschallinger, B., Vreugdenhil, M., 2023. Soil moisture retrieval from Sentinel-1 using a first-order radiative transfer model—a case-study over the Po-Valley. Remote Sens. Environ. 295, 113651. https://doi.org/10.1016/j.rse.2023.113651.

Rachdane, M., Saidi, M.E., El Khalki, E.M., Hadri, A., Boughdadi, S., Nehmadou, M., Ahbari, A., Tramblay, Y., 2024. Unraveling flood dynamics at sub-daily time scales in semi-arid to arid basins in south Morocco. Nat. Hazards. https://doi.org/10.1007/s11069-024-07022-0.

Refsgaard, J.C., van der Sluijs, J.P., Brown, J., van der Keur, P., 2006. A framework for dealing with uncertainty due to model structure error. Adv. Water Resour. 29, 1586–1597. https://doi.org/10.1016/j.advwatres.2005.11.013.

Renard, B., Kavetski, D., Kuczera, G., Thyer, M., Franks, S.W., 2010. Understanding predictive uncertainty in hydrologic modeling: the challenge of identifying input and structural errors. Water Resour. Res. 46. https://doi.org/10.1029/2009WR008328.

Salvatier, J., Wiecki, T.V., Fonnesbeck, C., 2016. Probabilistic programming in Python using PyMC3. PeerJ Comput. Sci. 2, e55. https://doi.org/10.7717/peerj-cs.55.

Sazib, N., Mladenova, I., Bolten, J., 2018. Leveraging the google earth engine for drought assessment using global soil moisture data. Remote Sens. 10, 1265. https://doi.org/10.3390/rs10081265.

Schilling, O.S., Cook, P.G., Brunner, P., 2019. Beyond classical observations in hydrogeology: the advantages of including exchange flux, temperature, tracer concentration, residence time, and soil moisture observations in groundwater model calibration. Rev. Geophys. 57, 146–182. https://doi.org/10.1029/2018RG000619.

Seibert, J., 2000. Multi-criteria calibration of a conceptual runoff model using a genetic algorithm. Hydrol. Earth Syst. Sci. 4, 215–224. https://doi.org/10.5194/hess-4-215-2000.

Seibert, J., 2001. On the need for benchmarks in hydrological modelling. Hydrol. Process 15, 1063–1064. https://doi.org/10.1002/hyp.446.

Shahrban, M., Walker, J.P., Wang, Q.J., Robertson, D.E., 2018. On the importance of soil moisture in calibration of rainfall–runoff models: two case studies. Hydrol. Sci. J. 63, 1292–1312. https://doi.org/10.1080/02626667.2018.1487560.

Siebert, S., Burke, J., Faures, J.M., Frenken, K., Hoogeveen, J., Döll, P., Portmann, F.T., 2010. Groundwater use for irrigation – a global inventory. Hydrol. Earth Syst. Sci. 14, 1863–1880. https://doi.org/10.5194/hess-14-1863-2010.

Sivelle, V., Jourde, H., Bittner, D., Richieri, B., Labat, D., Hartmann, A., Chiogna, G., 2022. Considering land cover and land use (LCLU) in lumped parameter modeling in forest dominated karst catchments. J. Hydrol. 612, 128264. https://doi.org/10.1016/j.jhydrol.2022.128264.

Stampoulis, D., Anagnostou, E.N., Nikolopoulos, E.I., 2013. Assessment of high-resolution satellite-based rainfall estimates over the mediterranean during heavy precipitation events. J. Hydrometeorol. 14, 1500–1514. https://doi.org/10.1175/JHM-D-12-0167.1.

Thébault, C., Perrin, C., Andréassian, V., Thirel, G., Legrand, S., Delaigue, O., 2023. MultiModel. Approach a Var. Spat. Framew. Streamflow Simul. (Prepr.). Catchment Hydrol. /Model. Approaches. https://doi.org/10.5194/egusphere-2023-569.

Tong, R., Parajka, J., Széles, B., Greimeister-Pfeil, I., Vreugdenhil, M., Komma, J., Valent, P., Blöschl, G., 2022. The value of satellite soil moisture and snow cover data for the transfer of hydrological model parameters to ungauged sites. Hydrol. Earth Syst. Sci. 26, 1779–1799. https://doi.org/10.5194/hess-26-1779-2022.

Tramblay, Y., Arnaud, P., Artigue, G., Lang, M., Paquet, E., Neppel, L., Sauquet, E., 2023a. Changes in Mediterranean flood processes and seasonality. Hydrol. Earth Syst. Sci. 27, 2973–2987. https://doi.org/10.5194/hess-27-2973-2023.

Tramblay, Y., El Khalki, E.M., Ciabatta, L., Camici, S., Hanich, L., Saidi, M.E.M., Ezzahouani, A., Benaabidate, L., Mahé, G., Brocca, L., 2023b. River runoff estimation with satellite rainfall in Morocco. Hydrol. Sci. J. 68, 474–487. https://doi.org/10.1080/02626667.2023.2171295.

Wagner, W., Hahn, S., Kidd, R., Melzer, T., Bartalis, Z., Hasenauer, S., Figa-Saldaña, J., de Rosnay, P., Jann, A., Schneider, S., Komma, J., Kubu, G., Brugger, K., Aubrecht, C., Züger, J., Gangkofner, U., Kienberger, S., Brocca, L., Wang, Y., Blöschl, G., Eitzinger, J., Steinnocher, K., 2013. The ASCAT Soil moisture product: a review of its specifications, validation results, and emerging applications. Meteorol. Z. 5–33. https://doi.org/10.1127/0941-2948/2013/0399.

Wagner, W., Lindorfer, R., Hahn, S., Kim, H., Vreugdenhil, M., Gruber, A., Fischer, M., Trnka, M., 2024. Global scale mapping of subsurface scattering signals impacting ASCAT soil moisture retrievals, 1–1 IEEE Trans. Geosci. Remote Sens.. https://doi.org/10.1109/TGRS.2024.3429550.

Wagner, W., Lindorfer, R., Melzer, T., Hahn, S., Bauer-Marschallinger, B., Morrison, K., Calvet, J.-C., Hobbs, S., Quast, R., Greimeister-Pfeil, I., Vreugdenhil, M., 2022. Widespread occurrence of anomalous C-band backscatter signals in arid environments caused by subsurface scattering. Remote Sens. Environ. 276, 113025. https://doi.org/10.1016/j.rse.2022.113025.

Wooldridge, S.A., Kalma, J.D., Walker, J.P., 2003. Importance of soil moisture measurements for inferring parameters in hydrologic models of low-yielding ephemeral catchments. Environ. Model. Softw. 18, 35–48. https://doi.org/10.1016/S1364-8152(02)00038-5.